Supplementary Data

Morphological tuning *via* structural modulations in AIE luminogens with least possible variables and their use in live cell imaging

Roop Shikha Singh,[a] Rakesh Kumar Gupta,[a] Rajendra Prasad Paitandi,[a] Mrigendra Dubey,[a] Gunjan Sharma,[b] Biplob Koch[b] and Daya Shankar Pandey*[a]

[a]Department of Chemistry, Faculty of Science, Banaras Hindu University, Varanasi - 221 005 (U.P.) India,

[b]Department of Zoology, Faculty of Science, Banaras Hindu University, Varanasi - 221 005 (U.P.) India

Contents

General Information

Elemental analyses for C, H and N were performed on an Exeter Analytical Inc. Model CE-440 CHN analyser. Infra-red and electronic absorption spectra were acquired on a Perkin Elmer-577 and Shimadzu UV-1601 spectrophotometers, respectively. ^{1}H, and ^{13}C spectra were acquired on a JEOL AL 300 FT-NMR using tetramethylsilane ($Si(CH_3)_4$) as an internal reference. Fluorescence spectra (95% aqueous-methanol) at room temperature was acquired on a Perkin-Elmer *LS* 55 Fluorescence spectrometer. High resolution mass spectra (HRMS) were obtained on THERMO Finningan LCQ Advantage Max ion trap mass spectrometer as described elsewhere.[1] Crystal data for **BQ1** and **BQ3** were collected on a Kappa Apex II CCD Duo diffractometer with graphite monochromated Mo-Ka radiation (0.71073 Å) at 100 K. An empirical multi-scan absorption correction was performed using SADABS. X-ray data for **BQ2** was collected on on a Bruker Kappa Apex-II diffractometer at RT with Mo-Kα radiation (λ = 0.71073 Å) and for **BQ4** on a dual source super nova CCD system from Agilent Technologies (Oxford Diffraction) at RT with Mo-Kα radiation (λ = 0.71073 Å). The structures were solved by direct methods (SHELXS 97) and refined by full-matrix least squares on F^2 (SHELX 97).[2] Non-hydrogen atoms were refined with anisotropic thermal parameters. Hydrogen atoms were geometrically fixed and refined using a riding model. Computer program PLATON was used for analysing interaction and stacking distances[3]. The CCDC deposition Nos. 1039757 (**BQ1**), 1039758 (**BQ2**), 1039759 (**BQ3**) and 1039760 (**BQ4**) contains supplementary crystallographic data for this paper.

Theoretical studies. Quantum chemical calculations were performmed at B3LYP Density Functional Theory (DFT) level using B3LYP/6-31G** for **BQ1–BQ4**.[4] All the geometry optimizations and frequency calculations (to verify a genuine minimum energy structure) were performed using Gaussian 09 suits of program.[5]

Experimental Section

Reagents. The solvents were dried and distilled prior to their use following standard literature procedures.[6] Pyrrole, trifluoroacetic acid, aniline, toludine, anisidine, 2,3-dichloro-5,6-dicyano-1,4-benzoquinone (DDQ), triethylamine and boron trifluoride diethyl etherate were procured from Sigma Aldrich India and used as received without further purifications.

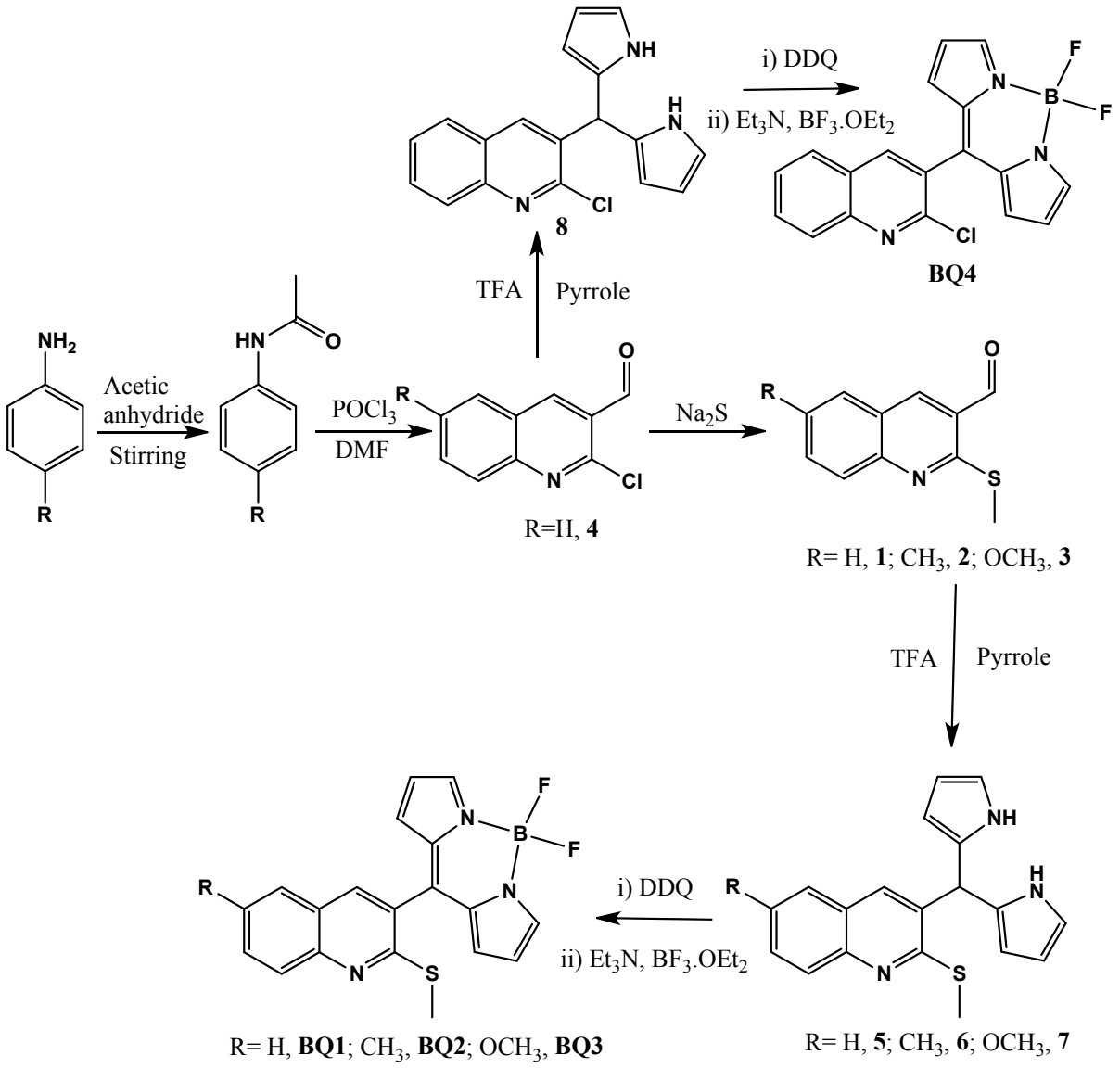

Scheme S1. Synthetic procedure for **5**–**8** and **BQ1**–**BQ4**.

Synthesis of compound 5. Pyrrole (10.0 ml) and catalytic amounts of trifluoroacetic acid (3 drops) were added to a flask containing compound **1** (1.5 g, 7.4 mmol) and contents of the flask was stirred at rt for 24 h. After completion of the reaction (monitored by TLC) the ensuing solution was concentrated to dryness under reduced pressure. Crude product thus obtained was purified by column chromatography (SiO_2; ethylacetate/hexane). Off white colored band was collected and concentrated to afford the desired product. Yield: 1.2 g, 80%. Analytical data: Anal. Calc. for $C_{19}H_{17}N_3S$: C, 71.44; H, 5.36; N, 13.15. Found: C, 71.23; H, 5.46; N, 13.04%. ^{1}H NMR ($CDCl_3$, δ ppm): 2.66 (3H, s, S-methyl), 5.81 (1H, s, methine-H), 5.90 (2H, s, pyrrolic-H), 6.17 (2H, s, pyrrolic-H), 6.70 (2H, s, pyrrolic-H), 7.37 (1H, t, aromatic-H), 7.60 (3H, m, aromatic-H), 7.94 (1H, d, J = 8.7 Hz, aromatic-H), 8.02 (2H, br, pyrrolic N-H proton. ^{13}C NMR ($CDCl_3$, δ ppm): 13.5, 39.8, 107.6, 108.7, 117.5, 125.2, 125.8, 127.6, 129.3, 130.7, 133.8, 134.4, 147.0, 159.2 and 199.9. IR (KBr pellets, cm^{-1}): 3378, 1619, 1594, 1564, 1493, 1445, 1346, 1219, 1169, 1090, 1028, 772 and 717.

Synthesis of compound 6. This compound was prepared by following the above procedure for **5** using aldehyde **2** (1.75 g, 8.00 mmol). Yield: 1.45 g, 83%. Analytical data: Anal. Calc. for $C_{20}H_{19}N_3S$: C, 72.04; H, 5.74; N, 12.60; Found C, 72.00; H, 5.53; N, 12.28%. ^{1}H NMR ($CDCl_3$, δ ppm): 2.47 (3H, t, methyl), 2.65 (3H, s, S-methyl), 5.77 (1H, s, methine-H), 5.87 (2H, s, pyrrolic-H), 6.15 (2H, s, pyrrolic-H), 6.67 (2H, s, pyrrolic -H), 7.41 (3H, s, aromatic-H), 7.83 (1H, d, J = 8.7 Hz, aromatic-H), 8.03 (2H, br, pyrrolic N-H proton. ^{13}C NMR ($CDCl_3$, δ ppm): 13.4, 21.3, 39.7, 107.6, 108.6, 117.4, 125.8, 126.5, 127.3, 130.8, 131.4, 133.4, 134.4, 134.9, 145.6 and 158.1. IR (KBr pellet, cm^{-1}): 3376, 1639, 1558, 1485, 1425, 1332, 1153, 1084, 1026, 819, 783, 729 and 559.

Synthesis of compound 7. It was prepared following the above procedure for **5** using aldehyde **3** (1.87 g, 8.00 mmol). Yield: 1.53 g, 82%. Analytical data: Anal. Calc. for $C_{20}H_{19}N_3OS$: C, 68.74; H, 5.48; N, 12.02; Found C, 68.52; H, 5.21; N, 12.00%. ^{1}H NMR ($CDCl_3$, δ ppm): 2.67 (3H, s, S-methyl), 3.93 (3H, s, O-methyl), 5.87 (3H, m, methine-H and pyrrolic -H), 6.19 (2H, s, pyrrolic-H), 6.76 (2H, s, pyrrolic-H), 6.90 (1H, s, aromatic-H), 7.71 (1H, m, aromatic-H), 8.13 (2H, d, aromatic-H), 8.57 (2H, br, pyrrolic N-H). ^{13}C NMR ($CDCl_3$, 75 MHz, δC, ppm): 13.5, 40.4, 55.6, 56.8, 106.5, 108.2, 117.1, 120.1, 120.7, 124.1, 131.5, 133.7,

138.4, 155.3, 163.3. IR (KBr pellet, cm^{-1}): 3379, 1638, 1568, 1483, 1425, 1328, 1153, 1094, 1028, 816, 787, 730 and 559.

Synthesis of compound 8. This compound was prepared following the above procedure for **5** using aldehyde **3** (1.52 g, 8.0 mmol). Yield: 1.24 g, 81.5%. Analytical data: Anal. Calc. for $C_{18}H_{14}ClN_3$: C, 70.24; H, 4.58; N, 13.65; Found C, 70.02; H, 4.14; N, 13.27%. ^{1}H NMR ($CDCl_3$, δ ppm): 5.86 (1H, s, methine-H) 5.93(2H, s, pyrrolic -H), 6.18 (2H, s, pyrrolic-H), 6.75 (2H, s, pyrrolic-H), 7.13 (2H, m, aromatic-H), 7.29 (2H, s, aromatic-H), 7.53 (2H, d, J = 9 Hz, aromatic-H), 7.68 (1H, s, aromatic-H), 8.13 (2H, br, pyrrolic N-H). ^{13}C NMR ($CDCl_3$, 75 MHz, δC, ppm): 40.7, 106.3, 107.7, 108.8, 117.6, 120.2, 122.5, 128.5, 130.6, 132.1, 137.4, 148.4, 161.2. IR (KBr pellet, cm^{-1}): 3369, 1626, 1532, 1481, 1409, 1336, 1149, 1063, 1016, 815, 788, 727 and 550.

Synthesis of BQ1. To a stirring solution of **5** (1.0 g, 3.1 mmol) dissolved in dichloromethane (15.0 mL), a solution of DDQ (0.703 g, 3.1 mmol) in benzene was added drop wise for an hour. The reaction mixture was stirred for additioal 2 h. After completion of the reaction contents of the flask was evaporated to dryness under reduced pressure. The crude product was dissolved in DCM and filtered to remove any solid impurities. Triethylamine (0.75 mL) and $BF_3.Et_2O$ (3.0 mL) were successively added to this solution and reaction mixture stirred for 15 min at rt. The progress of reaction was monitored by TLC. After completion of the reaction solution was filtered and filtrate was washed thrice with water, extracted with dichloromethane and concentrated to dryness under reduced pressure. Crude product thus obtained was charged on a flash column (SiO_2; CH_2Cl_2/hexane). The dark orange-red band was collected and concentrated to dryness to afford the desired product. Yield: 0.23 g, 23%. Analytical data: Anal. Calc. for $C_{19}H_{14}BF_2N_3S$: C, 62.49; H, 3.86; N, 11.51; Found C, 62.26; H, 3.49; N, 11.37%. ^{1}H NMR ($CDCl_3$, δ ppm): 2.64 (3H, s, S-methyl), 6.5 (2H, s, pyrrolic-H), 6.8 (2H, s, pyrrolic-H), 7.53 (1H, d, J = 6.6 Hz, aromatic-H), 7.78 (2H, d, J = 6.6 Hz, pyrrolic-H), 7.96 (3H, s, aromatic-H), 8.06 (1H, d, J = 6.9 Hz, aromatic-H). ^{13}C NMR ($CDCl_3$, δ ppm): 13.7, 35.5, 118.9, 124.3, 126.1, 127.9, 131.0, 135.4, 136.5, 145.3, 148.4, 150.2, 161.4 and 174.4. IR (KBr pellet, cm^{-1}): 3106, 2929, 1592, 1557, 1487, 1411, 1387, 1357, 1257, 1140, 1108, 975 and 764.

Synthesis of BQ2. It was prepared following the above procedure for **BQ1** using **6** (1.0 g, 3.0 mmol) in place of **5**. Yield: 0.27 g, 27%. Analytical data: Anal. Calc. for $C_{20}H_{16}BF_2N_3S$: C, 63.34; H, 4.25; N, 11.08; Found C, 63.09; H, 4.11; N, 10.87%. ^{1}H NMR ($CDCl_3$, δ ppm): 2.54

(3H, s, methylic-H), 2.62 (3H, s, S-methyl), 6.50 (2H, s, pyrrolic-H), 6.79 (2H, s, pyrrolic-H), 7.58 (2H, m, aromatic-H), 7.86 (2H, s, pyrrolic-H), 7.94 (2H, d, J = 7.8 Hz, aromatic-H). ^{13}C NMR ($CDCl_3$, δ ppm): 13.6, 21.5, 30.9, 118.8, 124.2, 126.0, 126.8, 127.7, 130.9, 133.2, 135.5 136.1, 145.2, 147.1, 157.2. IR (KBr pellet, cm^{-1}): 3108, 2922, 1589, 1557, 1489, 1387, 1356, 1257, 1107, 1073, 975 and 753.

Synthesis of BQ3. It was prepared following the above procedure for **BQ1** using **7** (1.0 g, 2.87 mmol) in place of **5**. Yield: 0.2 g, 20%. Analytical data: Anal. Calc. for $C_{20}H_{16}BF_2N_3OS$: C, 60.78; H, 4.08; N, 10.63; Found C, 60.37; H, 4.00; N, 10.16%. ^{1}H NMR ($CDCl_3$, δ ppm): 2.62 (3H, s, S-methyl), 3.93 (3H, s, O-methyl), 6.5 (2H, s, pyrrolic-H), 6.8 (2H, s, pyrrolic-H), 7.06 (1H, s, aromatic-H), 7.42 (1H, m, aromatic-H), 7.86 (2H, m, pyrrolic-H), 7.98 (2H, d, J = 10.8 Hz, aromatic-H). ^{13}C NMR ($CDCl_3$, δ ppm): 13.8, 49.8, 55.7, 97.5, 105.6, 118.9, 123.4, 129.4, 130.9, 135.4, 144.9, 155.4, 157.6, 165.5, 167.0 and 170.0. IR (KBr pellet, cm^{-1}): 3139, 2926, 1588, 1562, 1490, 1388, 1357, 1262, 1113, 1074, 951 and 785.

Synthesis of BQ4. It was prepared following the above procedure for **BQ1** using **8** (1.0 g, 3.25 mmol) in place of **5**. Yield: 0.21 g, 21%. Analytical data: Anal. Calc. for $C_{18}H_{11}BClF_2N_3$: C, 61.15; H, 3.14; N, 11.88; Found C, 61.01; H, 2.97; N, 11.37%. ^{1}H NMR ($CDCl_3$, δ ppm): 6.5 (2H, s, pyrrolic-H), 6.76 (2H, s, pyrrolic-H), 7.69 (1H, t, aromatic-H), 7.89 (2H, m, aromatic-H), 7.99 (2H, s, pyrrolic-H), 8.16 (1H, d, J = 8.4 Hz, aromatic-H), 8.26 (1H, s, aromatic-H). ^{13}C NMR ($CDCl_3$, δ ppm): 67.3, 89.4, 104.6, 119.3, 128.42, 130.8, 132.1, 140.1, 145.6, 147.2, 160.9, and 179.8. IR (KBr pellet, cm^{-1}): 3114, 2924, 1589, 1557, 1483, 1411, 1389, 1354, 1261, 1113, 1107, 973 and 759.

Cell imaging Experiment

Cell line and stock solution preparation. Dalton's Lymphoma (DL) cells were used for fluorescence study as well as cytotoxicity of the compounds. Murine cancer cell line was used and maintained by serial transplantation into peritoneal cavity of other mouse. Stock solution of the compounds were prepared in DMSO (100 mM) and diluted further by RPMI-1640 cell culture media.

Measurement of cytotoxicity by MTT assay: MTT assay has been assessed to evaluate the toxicity of **BQ1**–**BQ3** on live DL cells before fluorescence imaging. In this assay, DL cells

(40,000) were seeded in 96 well plates and exposed with increasing concentrations of the compounds (10, 25, 50, 75, 100, 150, 200 μM) for 24 h. Cells were then washed with PBS and incubated with 10 μL of MTT (stock solution, 5mg/mL) for 2 h. 150 μL DMSO was added in each well and incubated further for 30 min followed by optical density (O.D.) measurements.

Fluorescence cell imaging:

DL cells were chosen as a model for live cell tracking to explore the applicability of **BQ1**–**BQ3** as bio-probes for *in vitro* cell imaging. Two sets of experiments has been carried out, in the first set DL (1×10^6) cells were incubated with 20 μM of **BQ1**–**BQ3** for 2h. In another set, cells were pre incubated (for 2 h) with **BQ1**–**BQ3**, washed with PBS (phosphate-buffered saline) followed by staining with Hoechst 33342 for 20 min at room temperature in dark. Again, cells were washed and images acquired with fluorescence microscope (Nikon) at 20X magnification.

Results:

Cytotoxicity assay:

The cytotoxicity of compounds **BQ1**–**BQ3** was evaluated by using MTT assay to determine the metabolic viability of the DL cells. On the basis of O.D. it can be inferred that viability of the cells are not affected by the compounds. As shown in Figure S30, the DL cells grew normally in culture medium containing compounds in the concentration range of 10–200 μM, with almost no effect on the its physiology and proliferation.

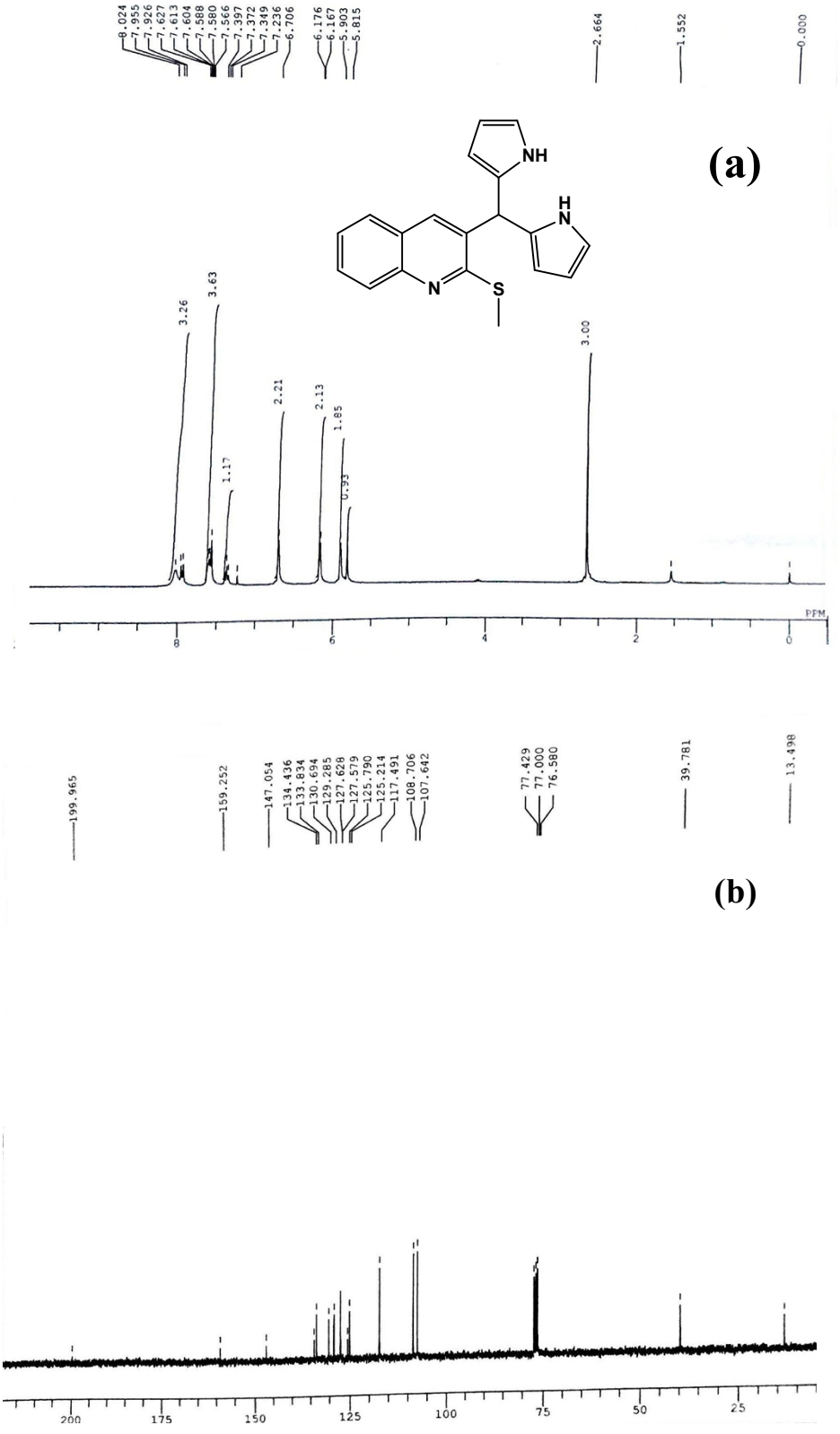

Figure S1. ^{1}H (a) and ^{13}C (b) NMR spectra of **5** in $CDCl_3$.

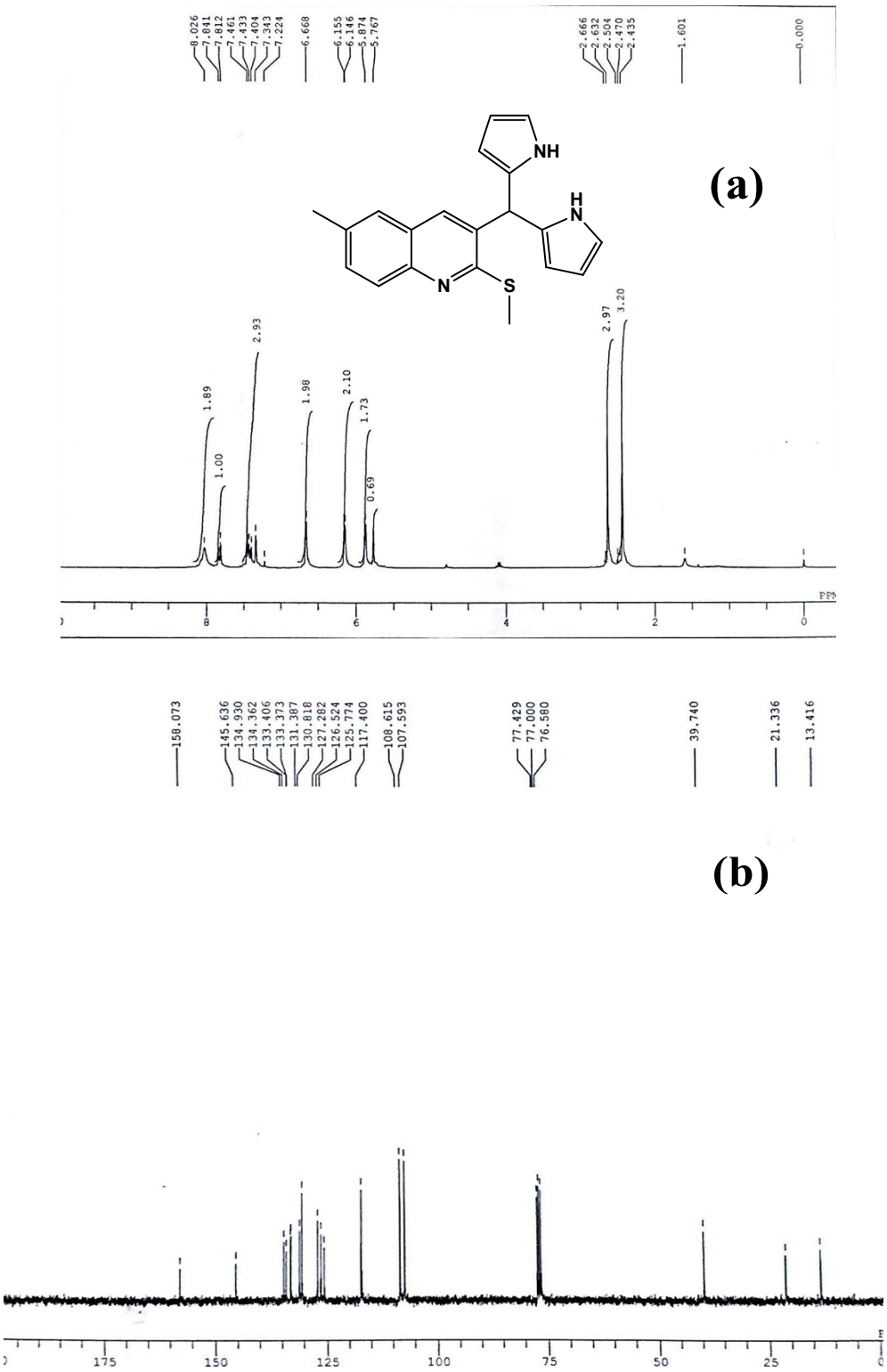

Figure S2. ^{1}H (a) and ^{13}C (b) NMR spectra of **6** in $CDCl_3$.

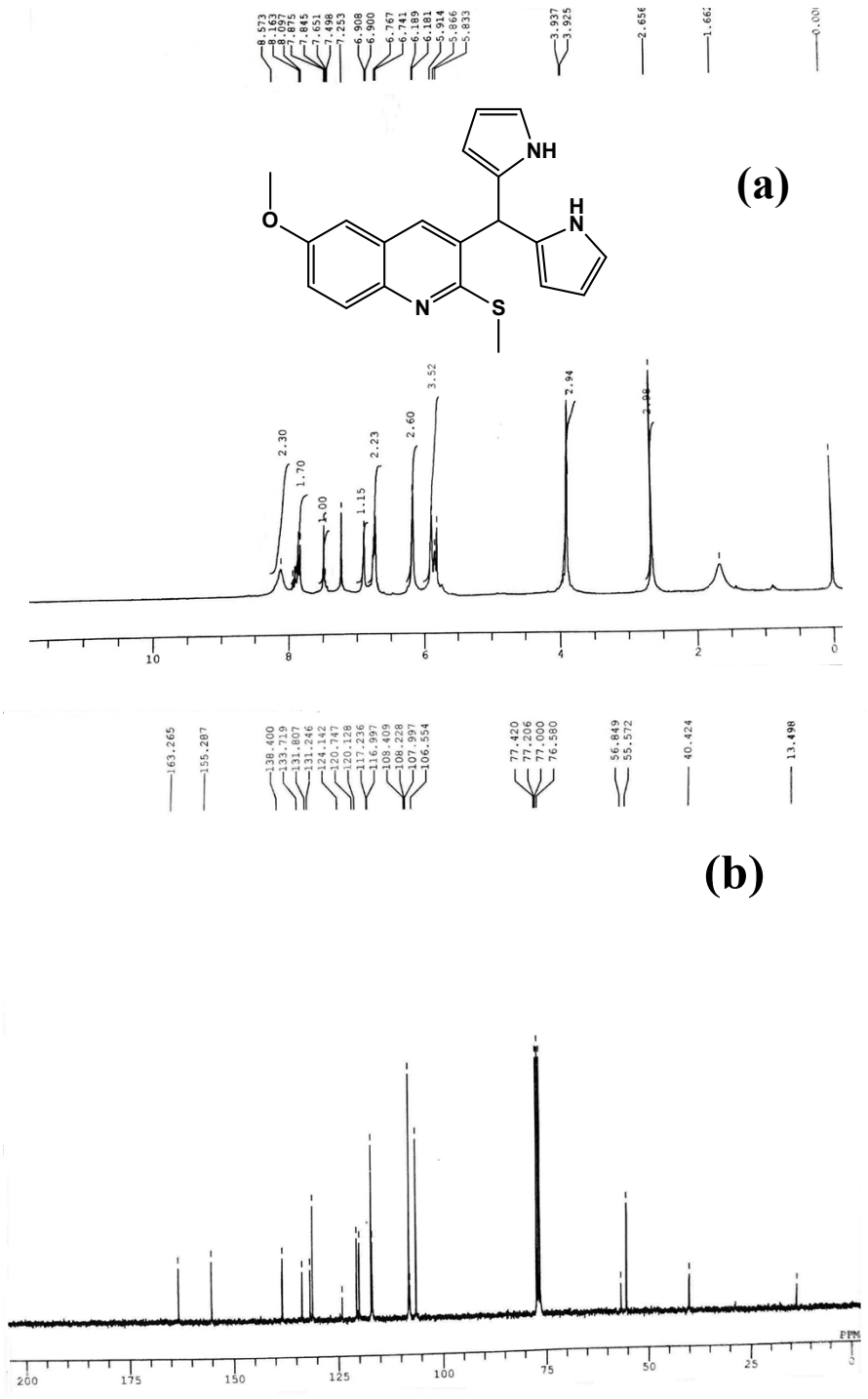

Figure S3. ^{1}H (a) and ^{13}C (b) NMR spectra of **7** in $CDCl_3$.

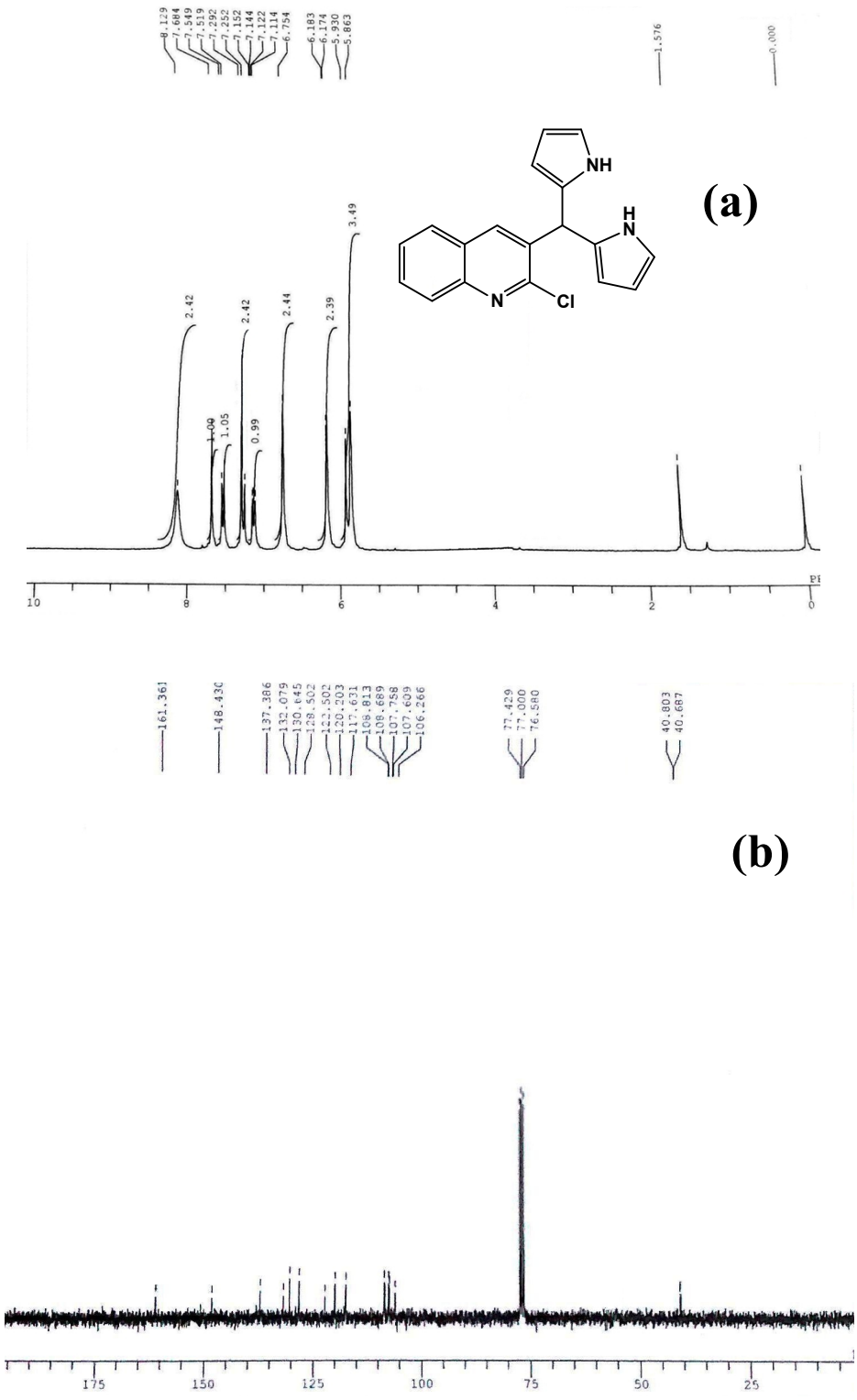

Figure S4. ^{1}H (a) and ^{13}C (b) NMR spectra of **8** in $CDCl_3$.

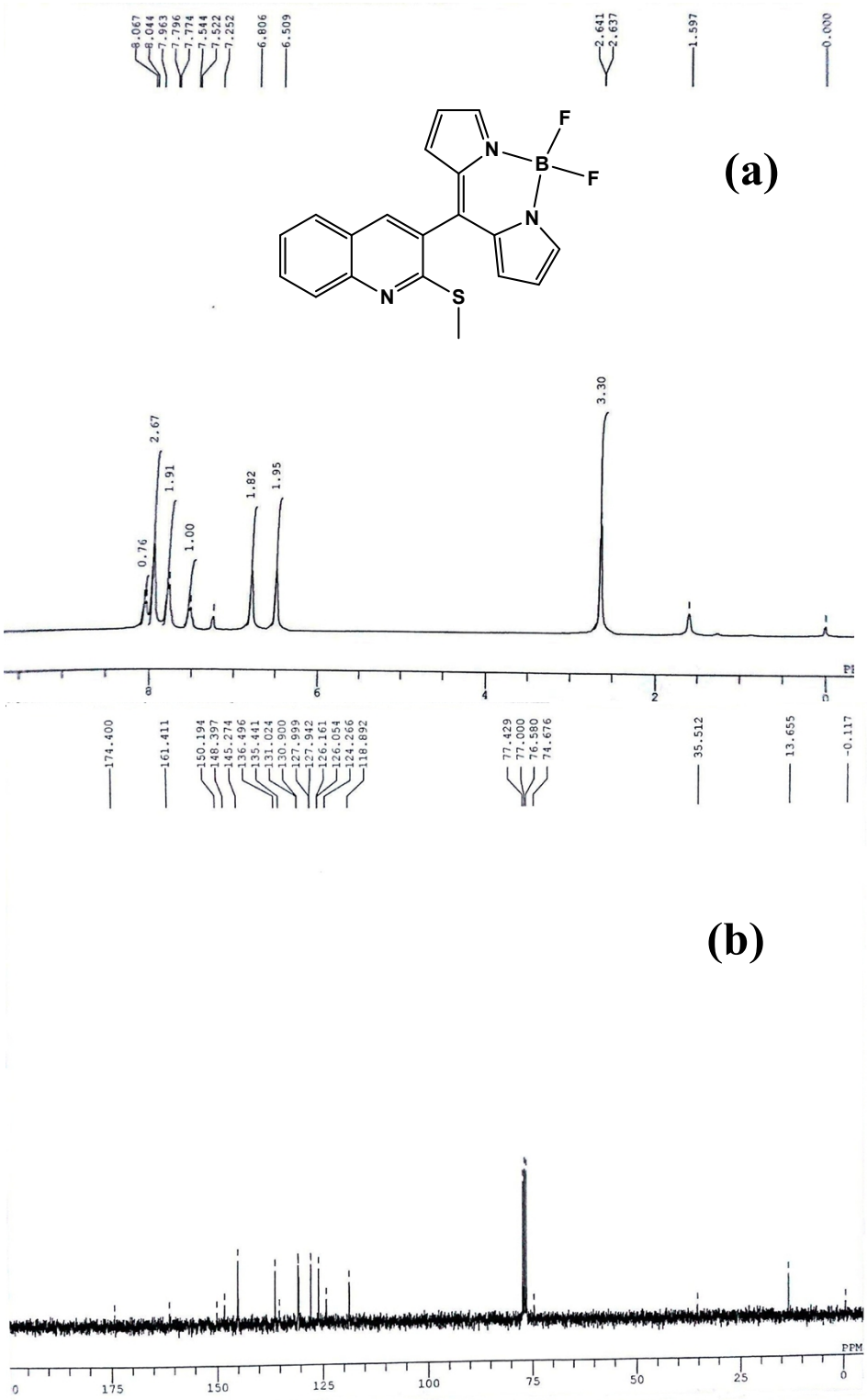

Figure S5. ^{1}H (a) and ^{13}C (b) NMR spectra of **BQ1** in $CDCl_3$.

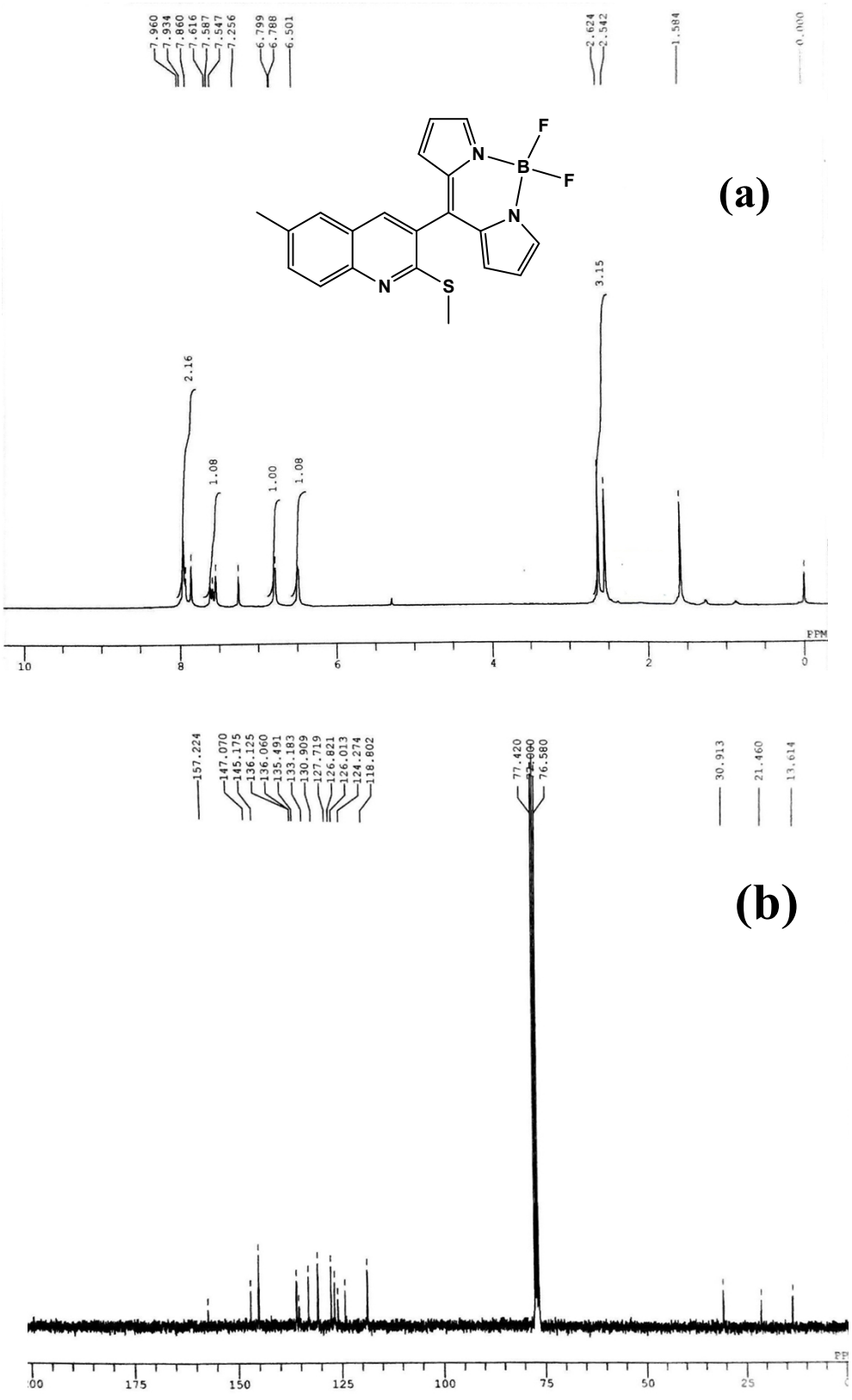

Figure S6. ^{1}H (a) and ^{13}C (b) NMR spectra of **BQ2** in $CDCl_3$.

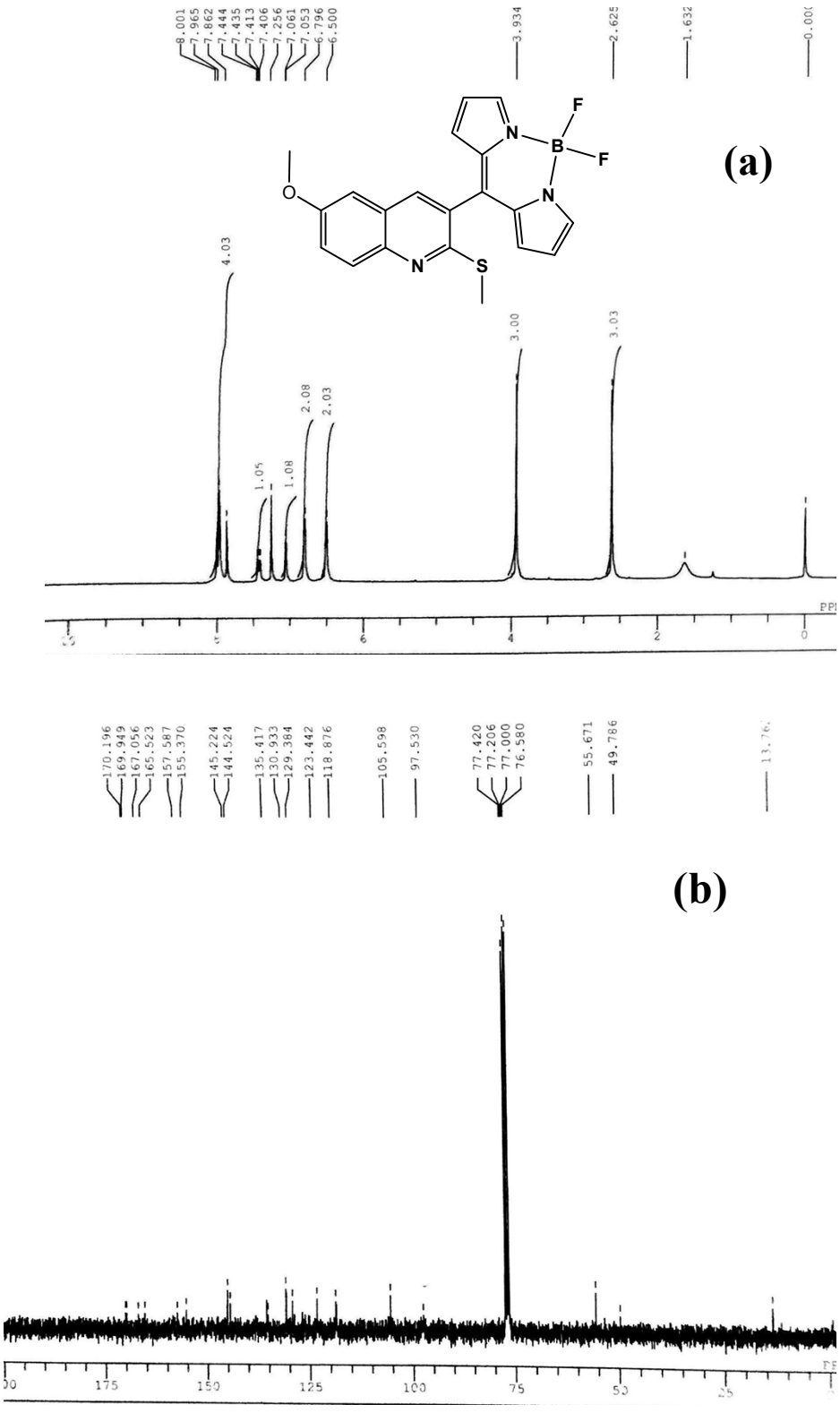

Figure S7. ^{1}H (a) and ^{13}C (b) NMR spectra of **BQ3** in $CDCl_3$.

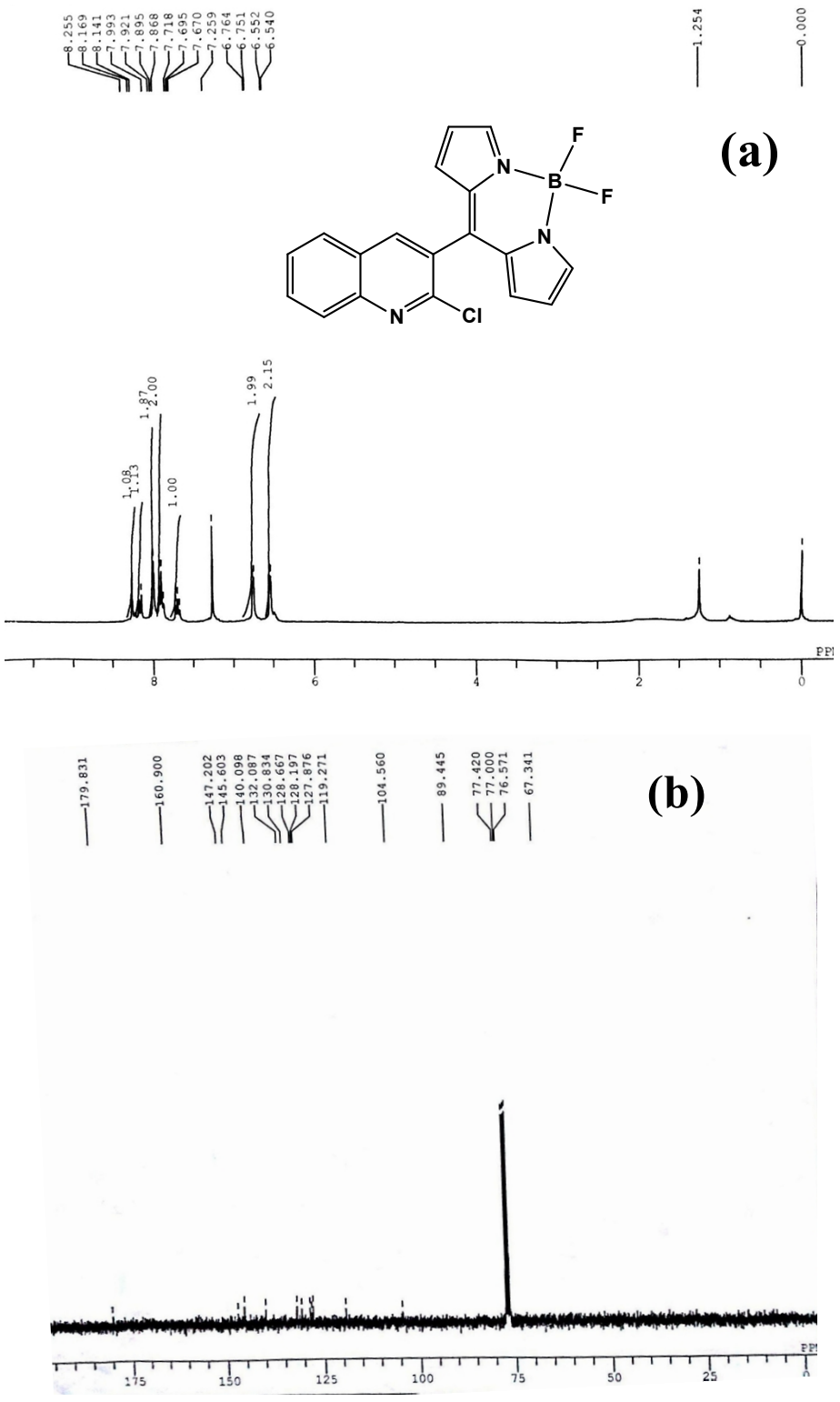

Figure S8. ^{1}H (a) and ^{13}C (b) NMR spectra of **BQ4** in $CDCl_3$.

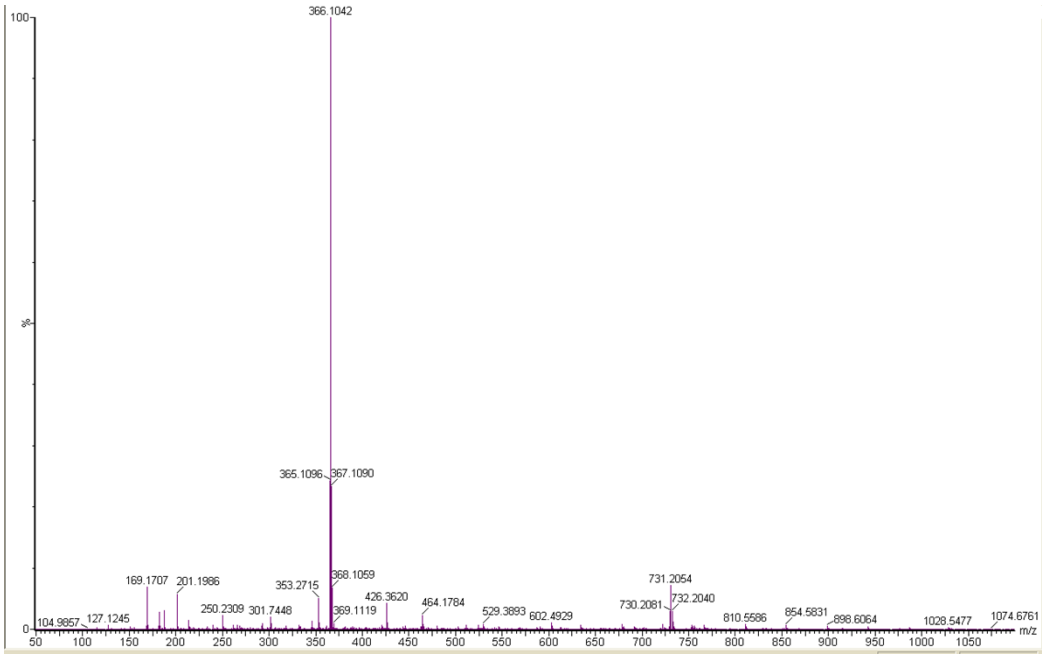

(a)

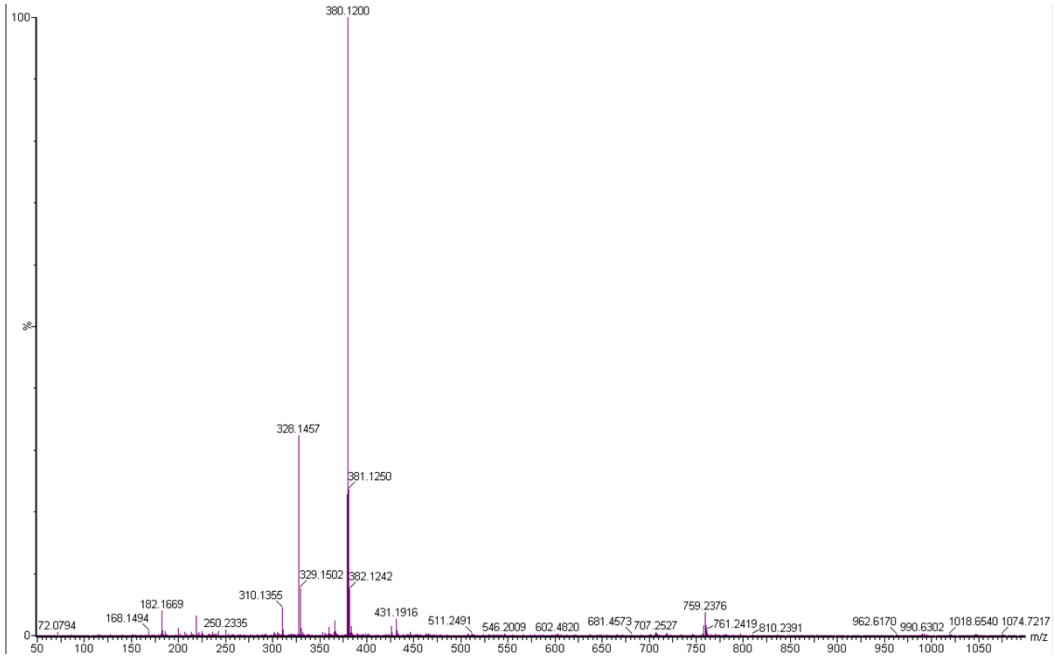

(b)

Figure S9. HRMS of **BQ1** (a) and **BQ2** (b).

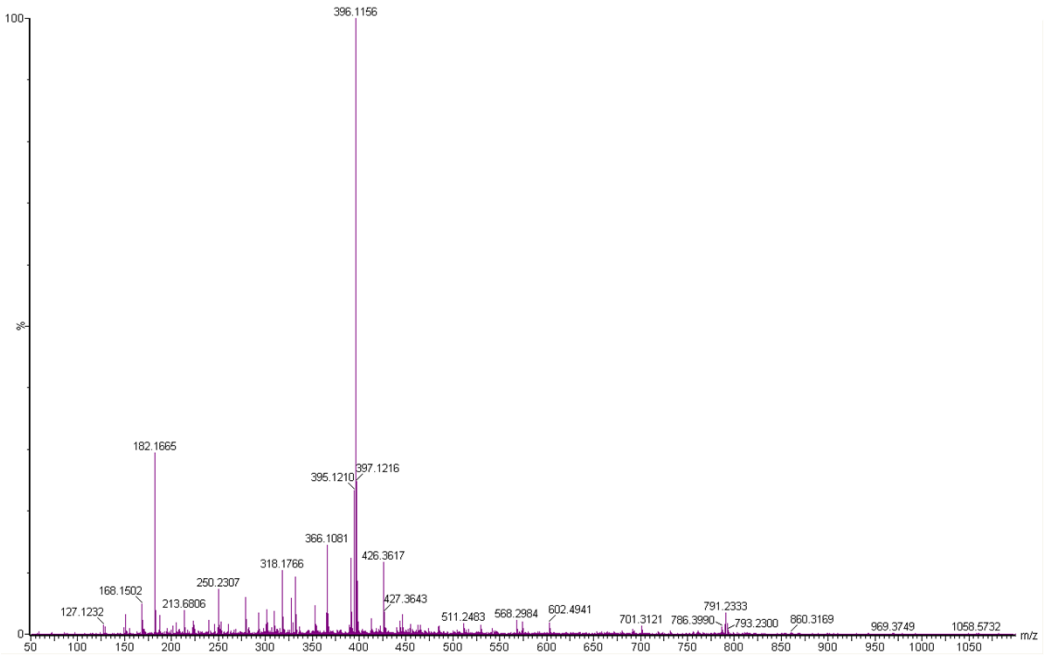

Figure S10. HRMS of **BQ3**.

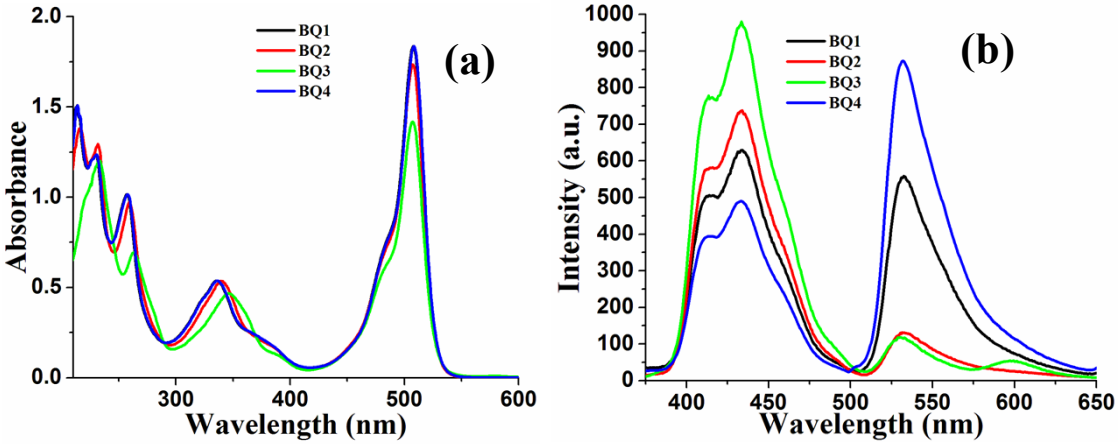

Figure S11. Absorption (a) and emission (b) spectra of **BQ1**–**BQ4** in methanol (*c*, 50 μM, λ_{ex} ~ 340 nm).

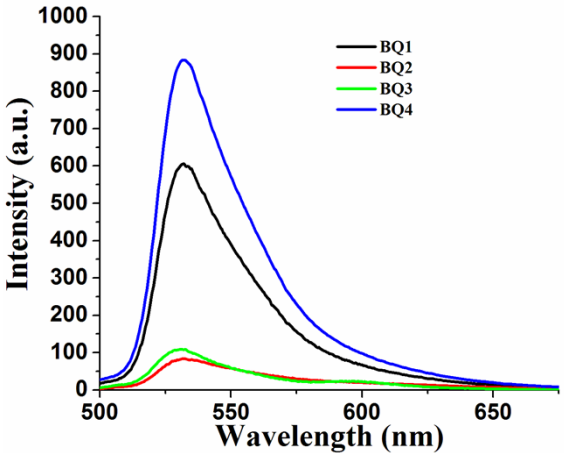

Figure S12. Emission spectra of **BQ1**–**BQ4** in methanol (*c*, 50 μM, λ_{ex} ~ 507 nm).

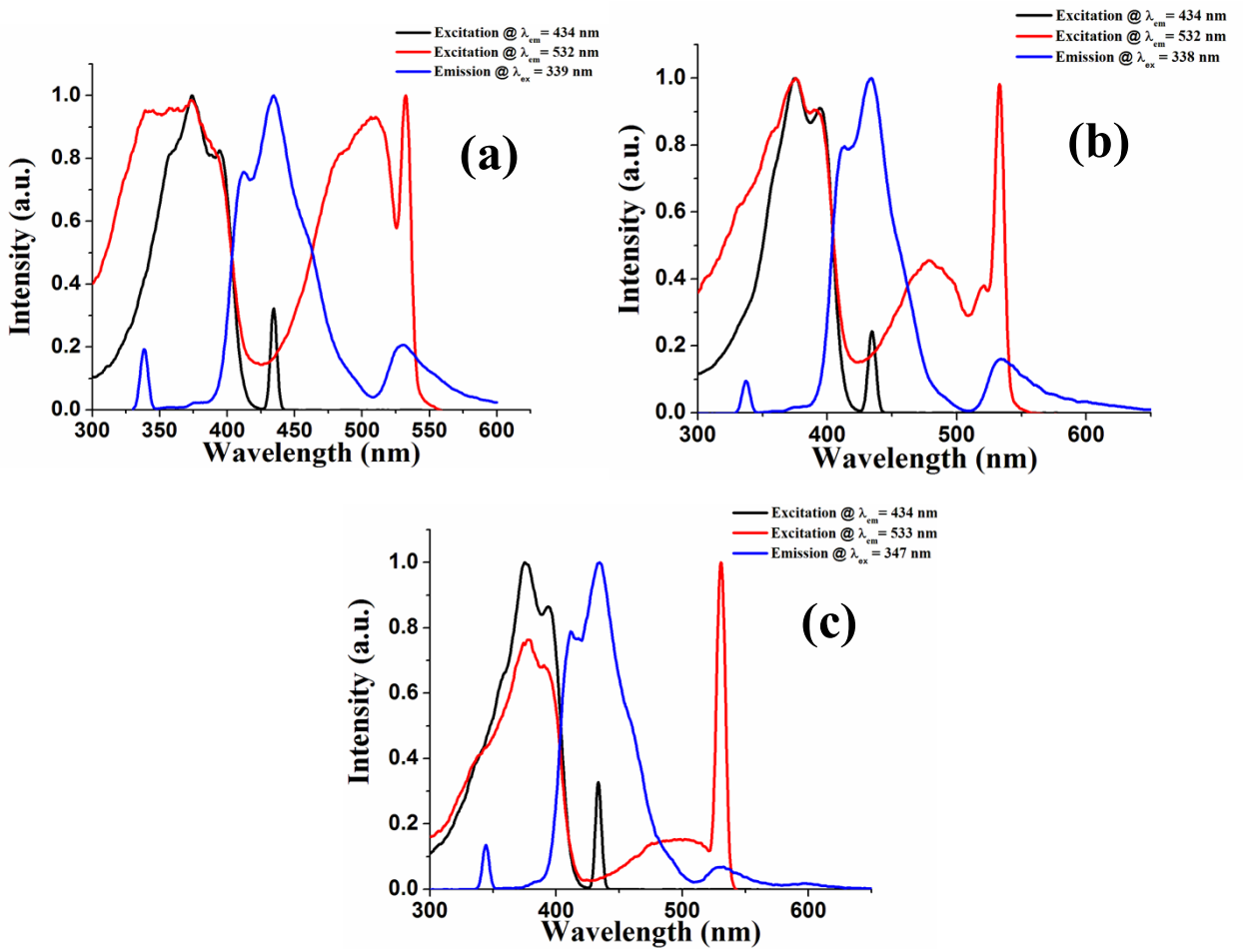
Excitation @ λem = 434 nm
Excitation @ λem = 532 nm
Emission @ λex = 339 nm
(a)
Intensity (a.u.)
Wavelength (nm)
Excitation @ λem = 434 nm
Excitation @ λem = 532 nm
Emission @ λex = 338 nm
(b)
Intensity (a.u.)
Wavelength (nm)
Excitation @ λem = 434 nm
Excitation @ λem = 533 nm
Emission @ λex = 347 nm
(c)
Intensity (a.u.)
Wavelength (nm)

Figure S13. Excitation spectra of **BQ1** (a), **BQ2** (b) and **BQ3**(c).

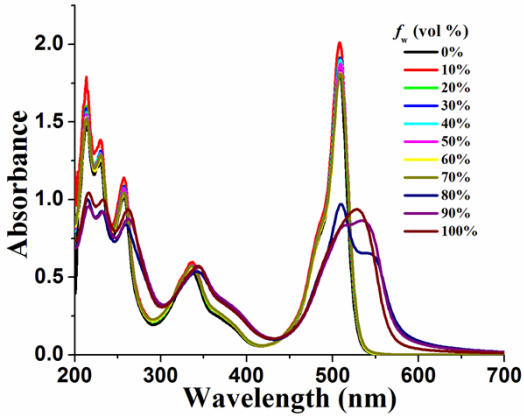

Figure S14. UV-vis spectra of **BQ1** (*c*, 50 μM) in methanol/water mixture with different volume fractions of water (f_W).

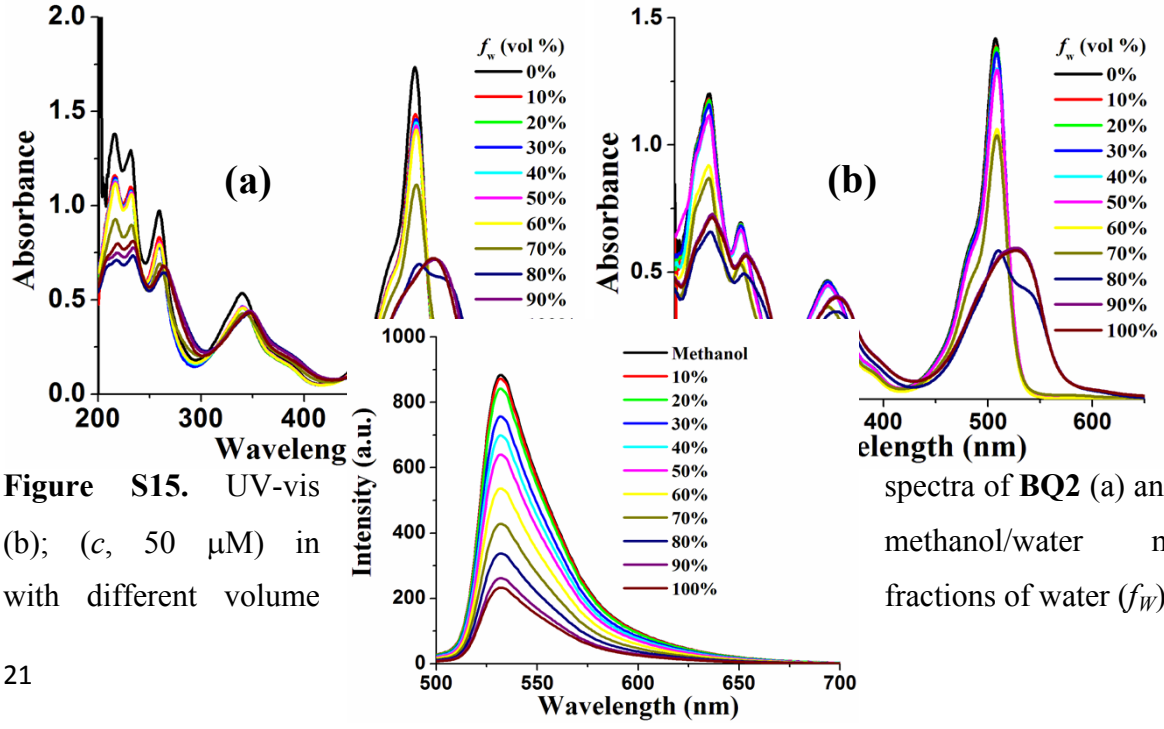

Figure S15. UV-vis spectra of **BQ2** (a) and **BQ3** (b); (*c*, 50 μM) in methanol/water mixture with different volume fractions of water (f_W).

Figure S16. Fluorescence spectra of **BQ4**(*c*, 50 μM) at λ_{ex} 508 nm in methanol/water mixture with different volume fractions of water (f_W).

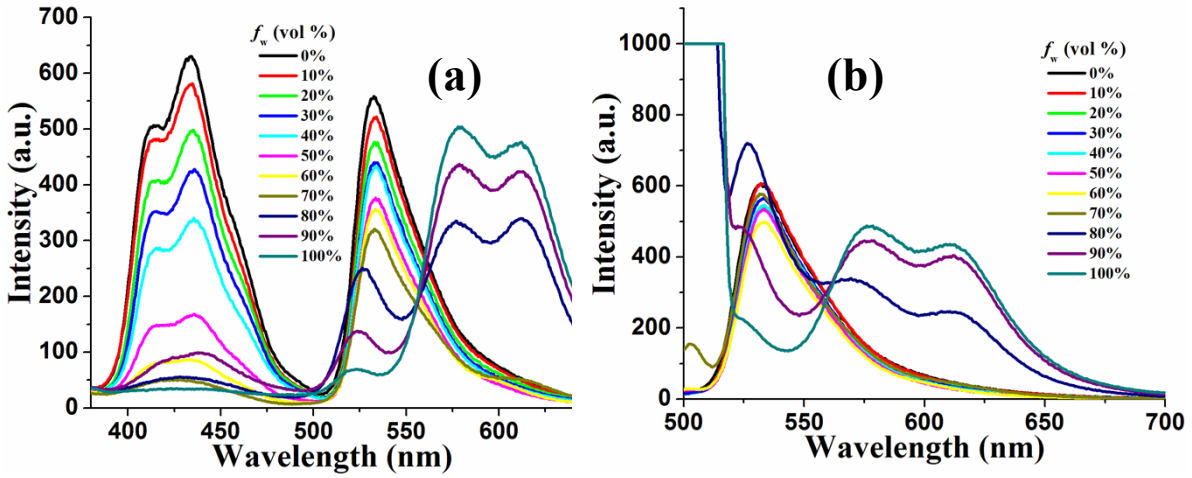

Figure S17. Fluorescence spectra of **BQ1** (*c*, 50 μM) at λ_{ex} 336 nm (a) and λ_{ex} 507 nm (b) in methanol/water mixture with different volume fractions of water (f_W).

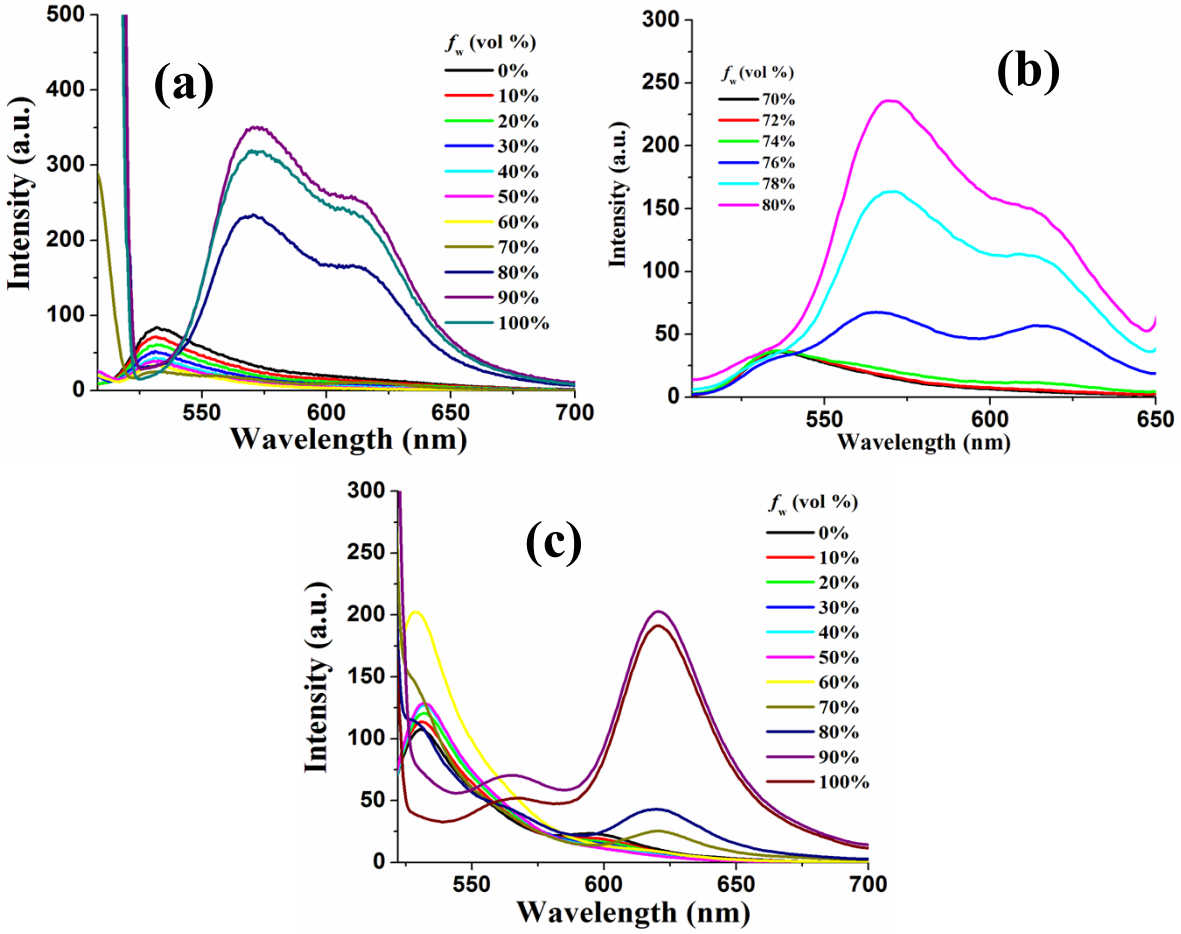

Figure S18. Fluorescence spectra of **BQ2** (c = 50 μM) (a) and **BQ3** (c, 50 μM) (b) in methanol/water mixture with different volume fractions of water (f_W), λ_{ex} 507 nm.

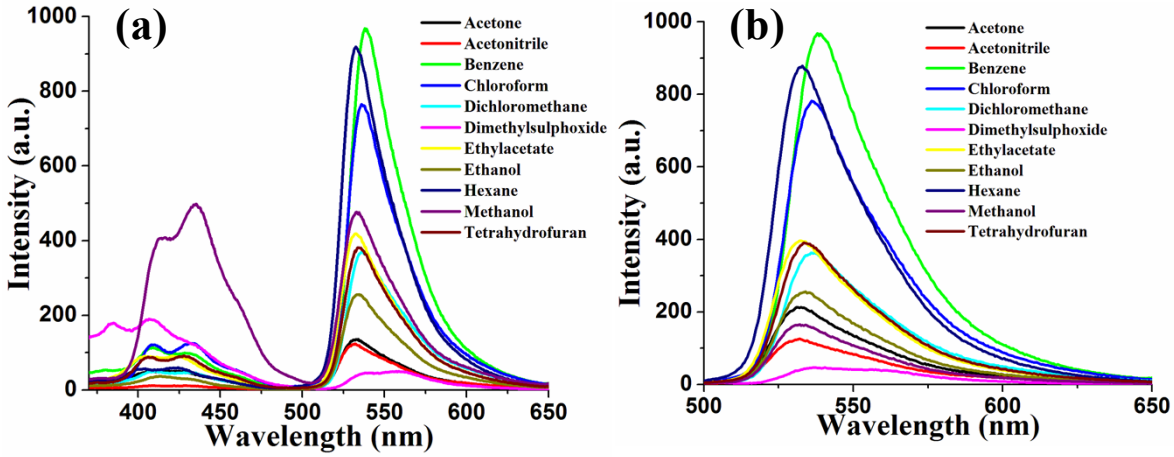

Figure S19. Fluorescence spectra of **BQ1** (*c*, 50 μM) at λ_{ex} 336 nm (a) and λ_{ex} 507 nm (b) in solvents with different polarities.

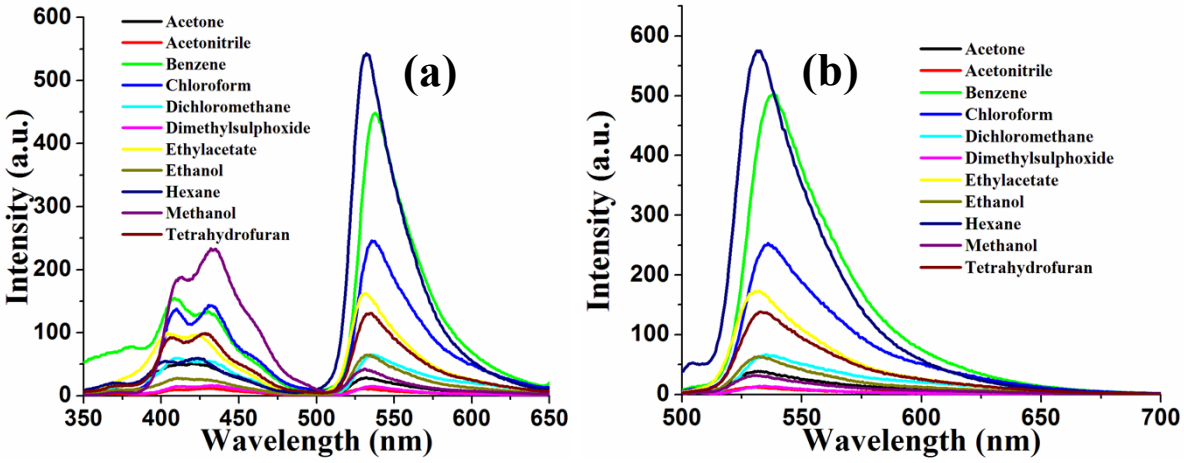

Figure S20. Fluorescence spectra of **BQ2** (*c*, 50 μM) at λ_{ex} 338 nm (a) and λ_{ex} 507 nm (b) in solvents with different polarities.

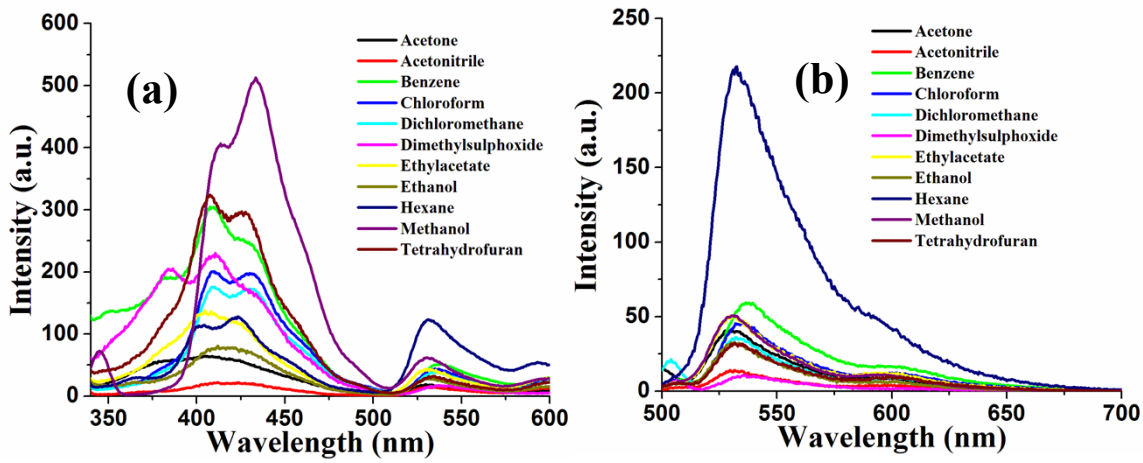

Figure S21. Fluorescence spectra of **BQ3** (*c*, 50 μM) at λ_{ex}, 345 nm (a) and λ_{ex}, 507 nm (b) in solvents with different polarities.

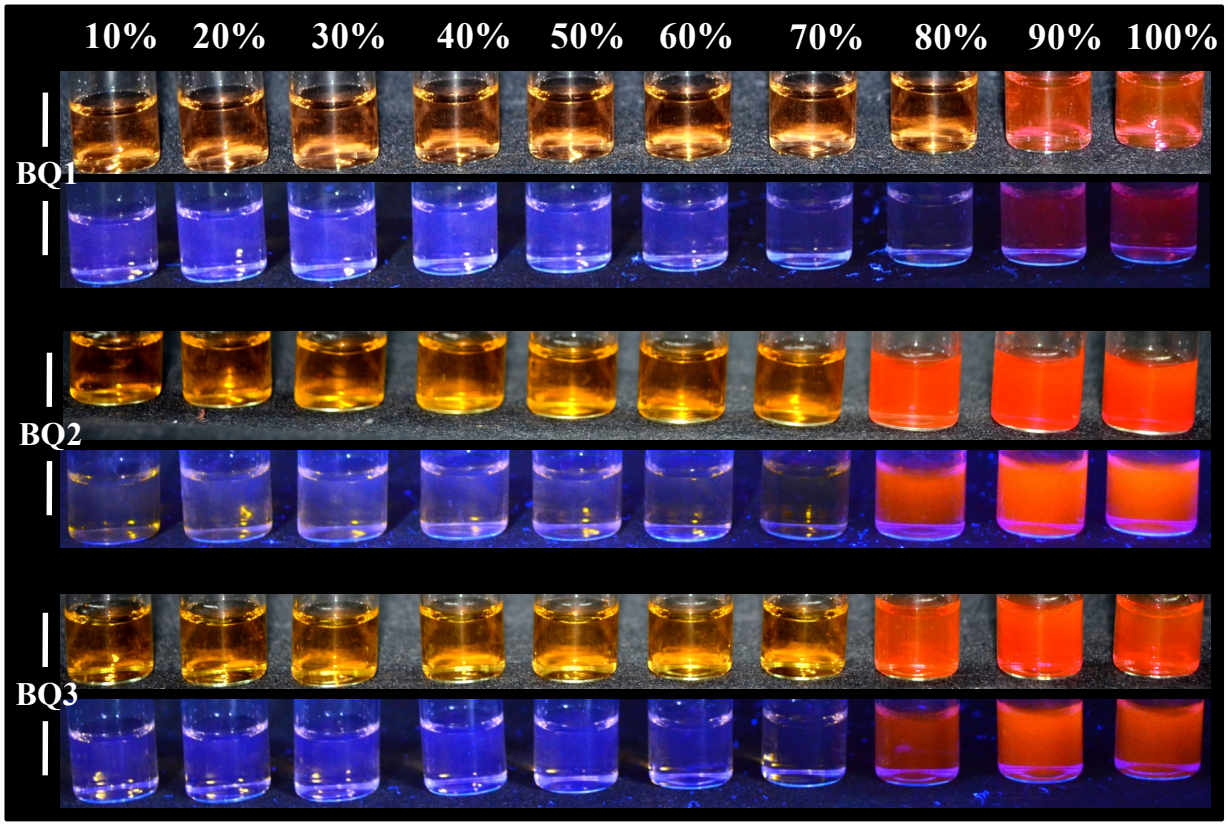

Figure S22. Photographs of **BQ1-BQ3** (*c*, 100 μM) showing visible color change under normal light (top) and UV illumination, λ_{ex} = 365 nm (bottom).

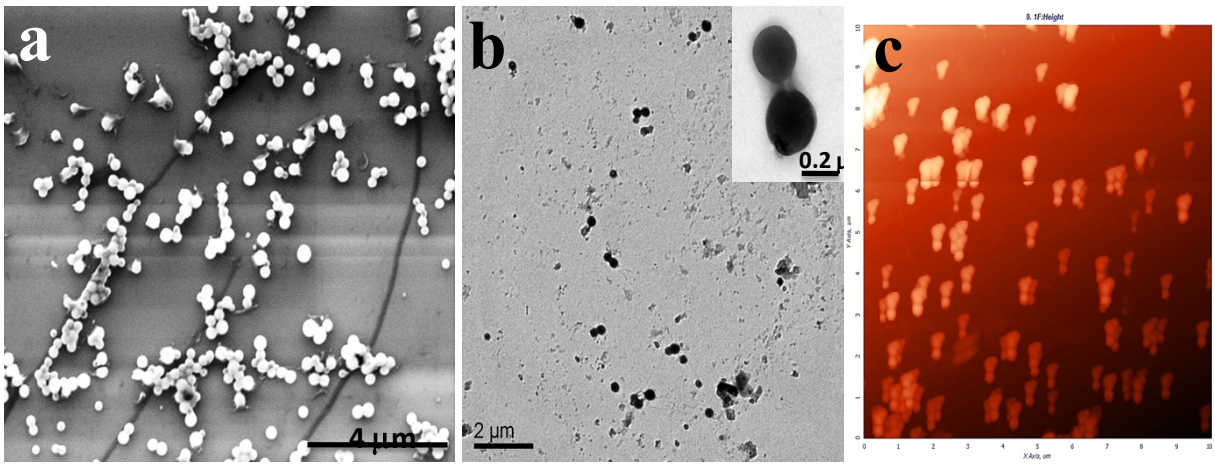

Figure S23. SEM (a); TEM (b) and AFM (c) images showing morphology of nanoaggregates of **BQ1** at *c*, 50 μM with f_W, 90%.

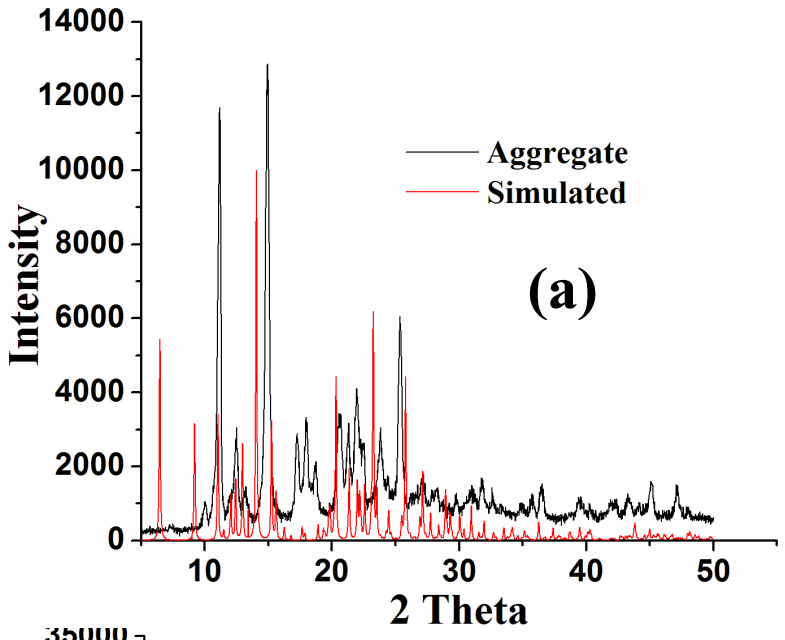

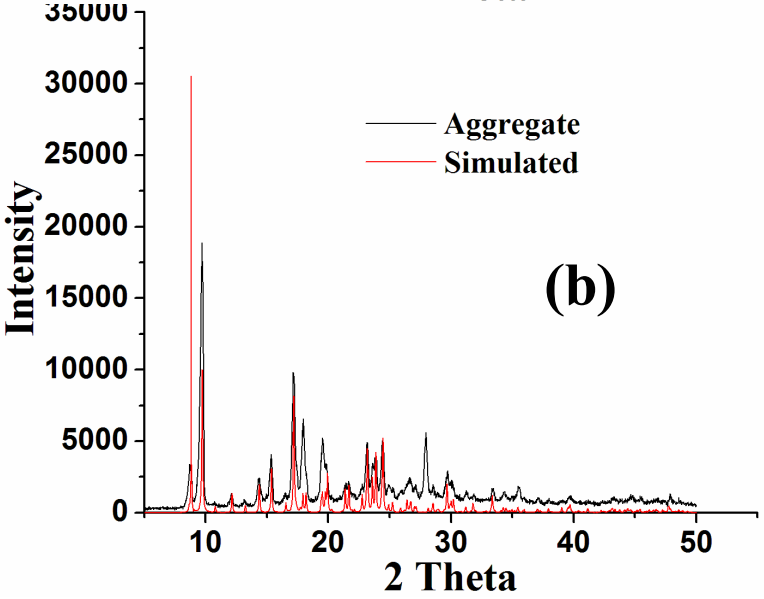

Figure S24. SEM image showing morphology of nanoaggregates of **BQ3** at *c*, 50 μM with f_W, 60%.

Figure S25. Powder XRD pattern of **BQ2** (a) and **BQ3** (b).

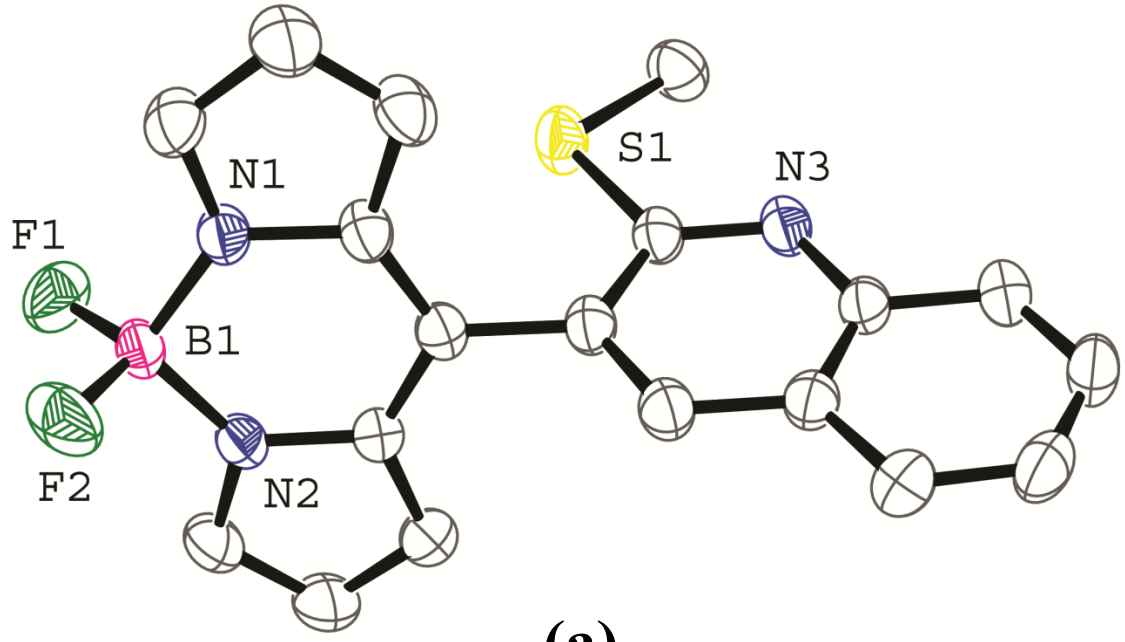

(a)

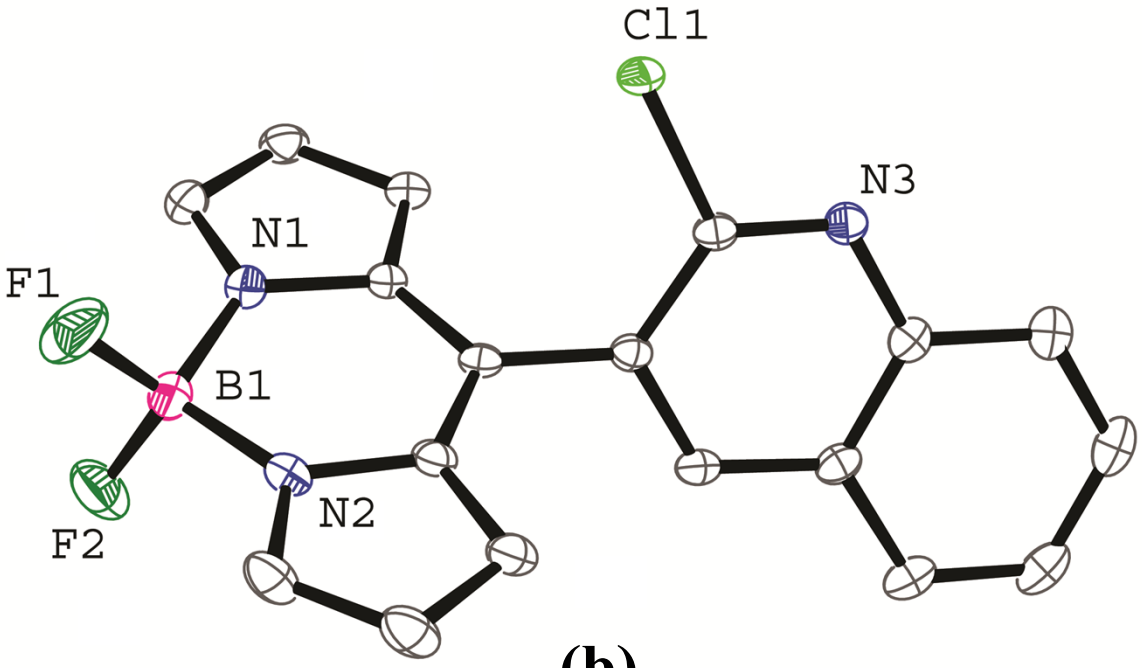

(b)

Figure S26. ORTEP view of **BQ1** (a) and **BQ4** (b) at 40% ellipsoidal probability.

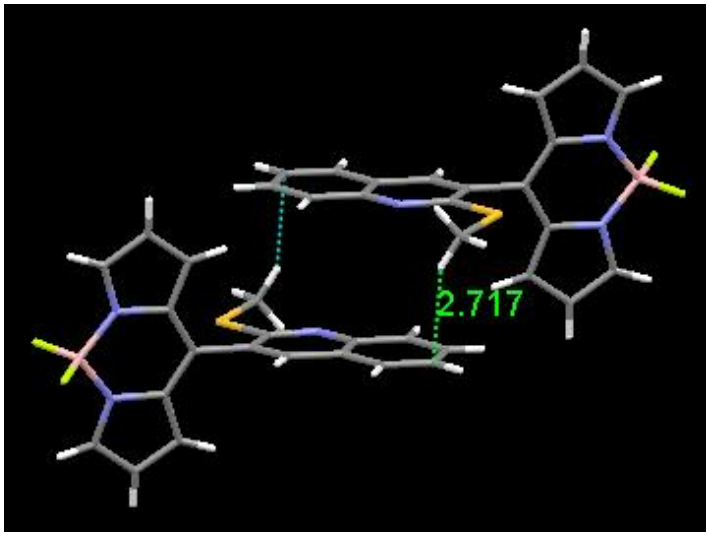

(a)

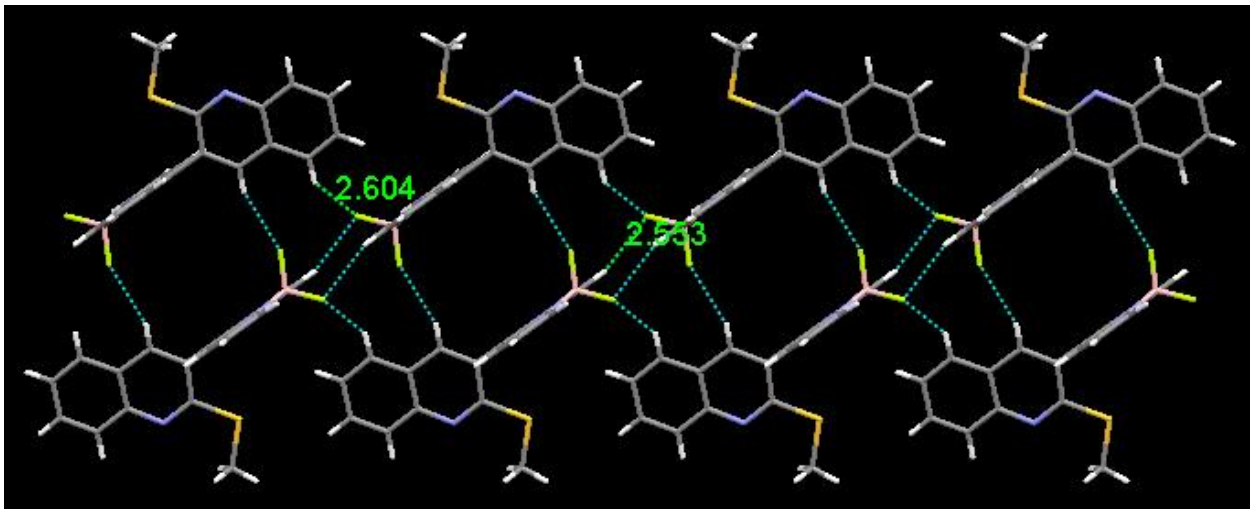

(b)

Figure S27. Intermolecular H-bonds {C–H···π (a) and C–H···F (b)} in **BQ1**.

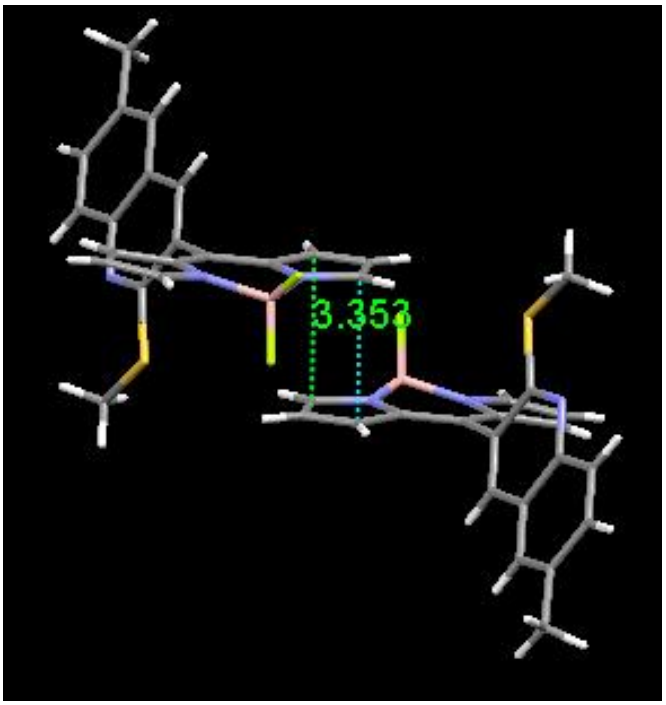

Figure S28. Partial view of the crystal packing through π–π stacking in **BQ2**.

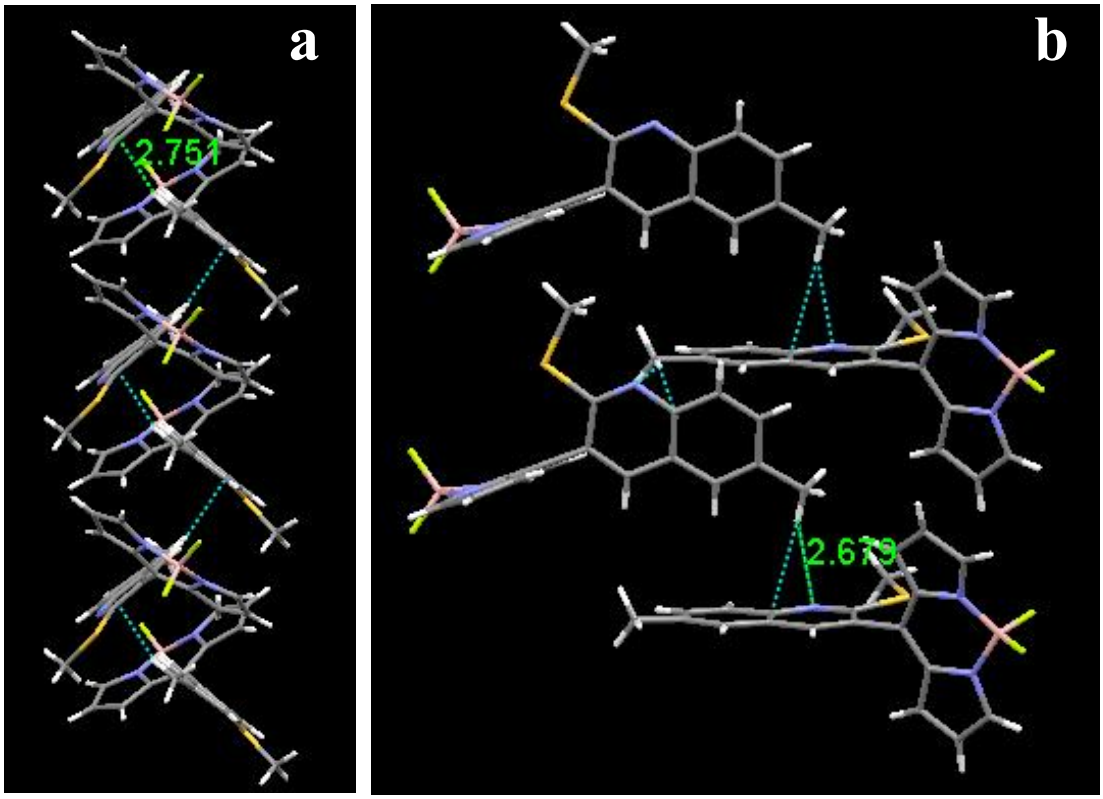

Figure S29. Intermolecular H-bonds {C–H···π (a) and C–H···N (b)} in **BQ2**.

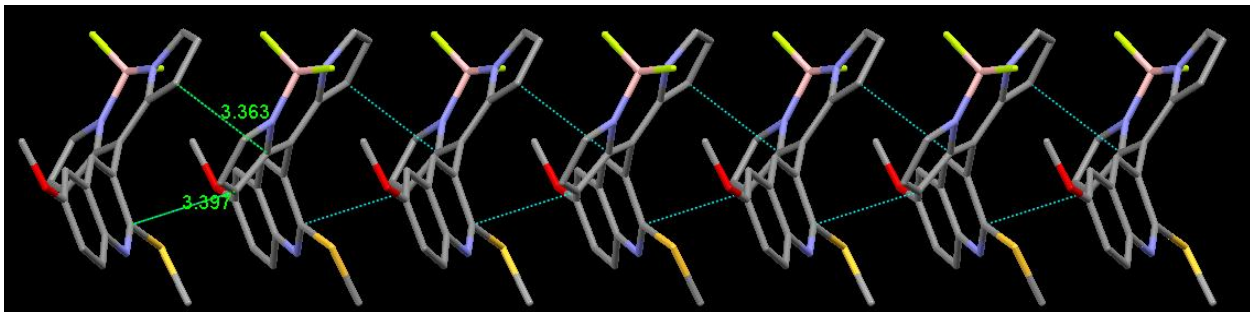

Figure S30. Partial view of the crystal packing through π–π stacking in **BQ3**.

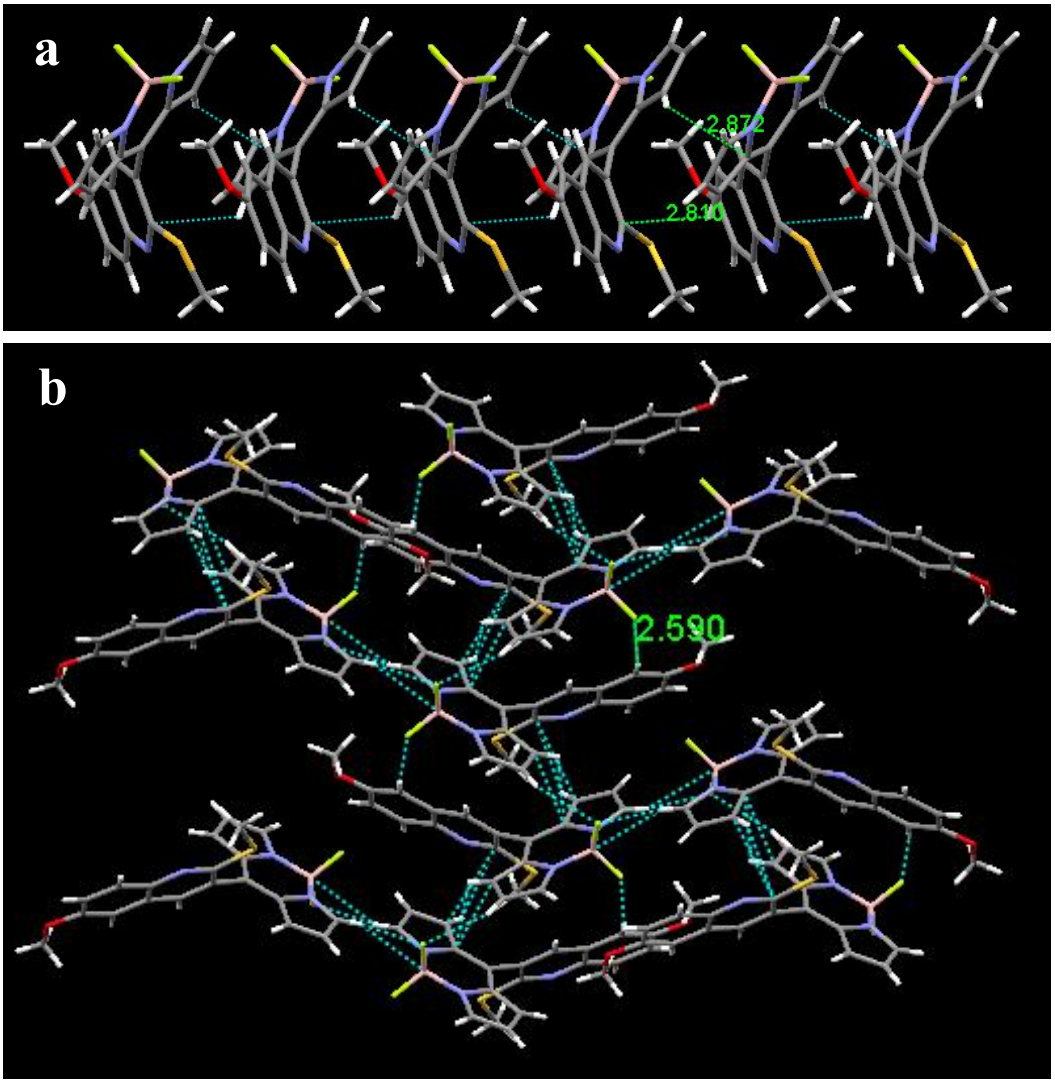

Figure S31. Intermolecular H-bonds {C–H···π (a) and C–H···F (b)} in **BQ3**.

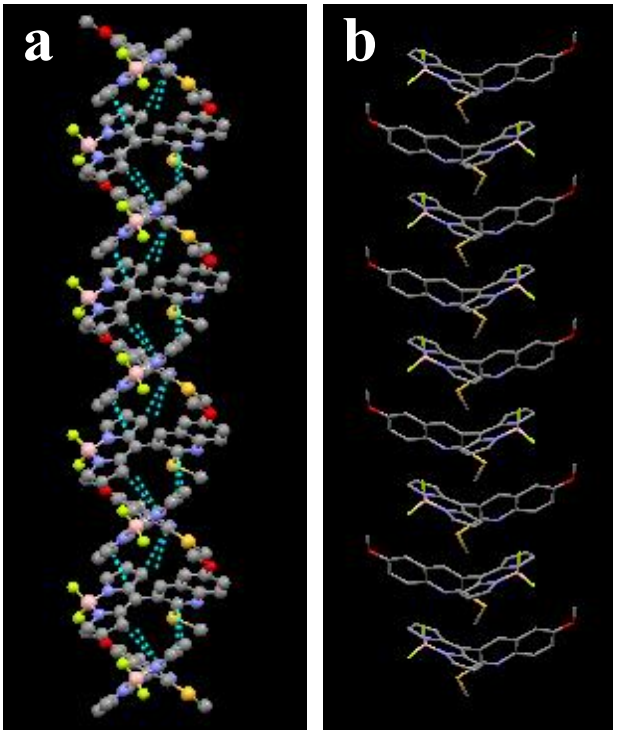

Figure S32. Double helical packing (a) and herringbone model (b) in **BQ3**.

Figure S33. Molecular orbital plots (HOMO and LUMO) and band gap of **BQ1**–**BQ3** for ground state.

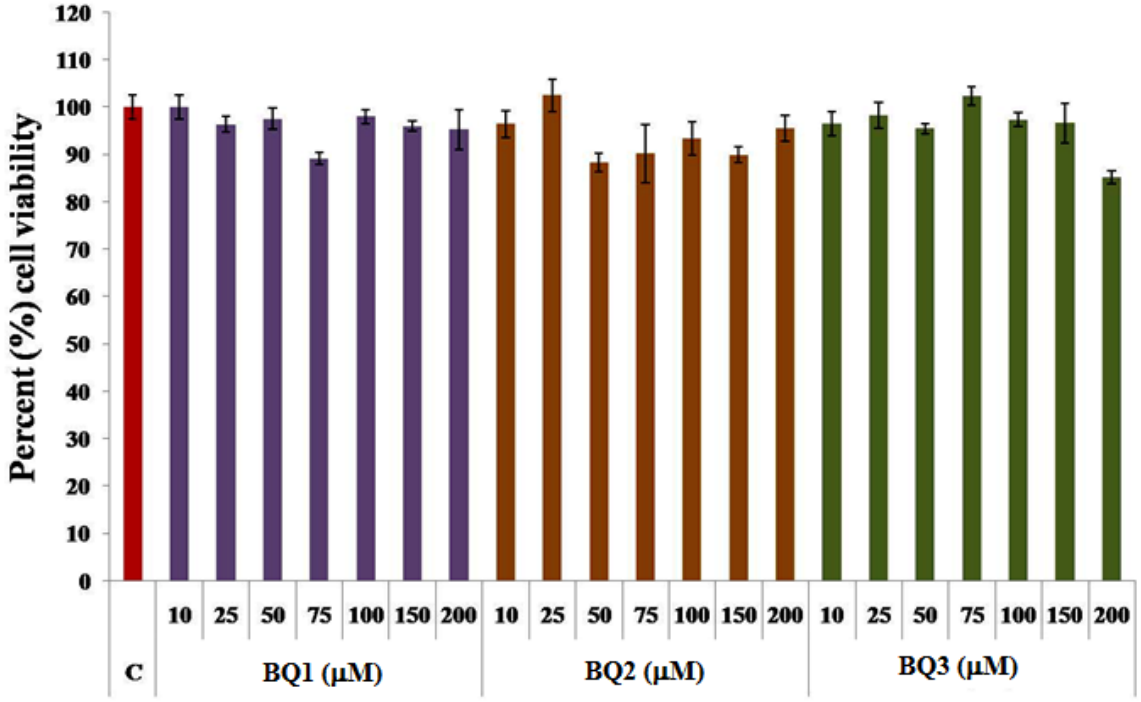

Figure S34. Cytotoxicity and cell proliferation effect of **BQ1**–**BQ3** were tested by MTT assay. DL cells were incubated with 10 to 200 µM concentrations of probes for 24 h. The absorbance measured at 570 nm is directly proportional to the number of living cells in the culture.

Probe excluded Nucleus:

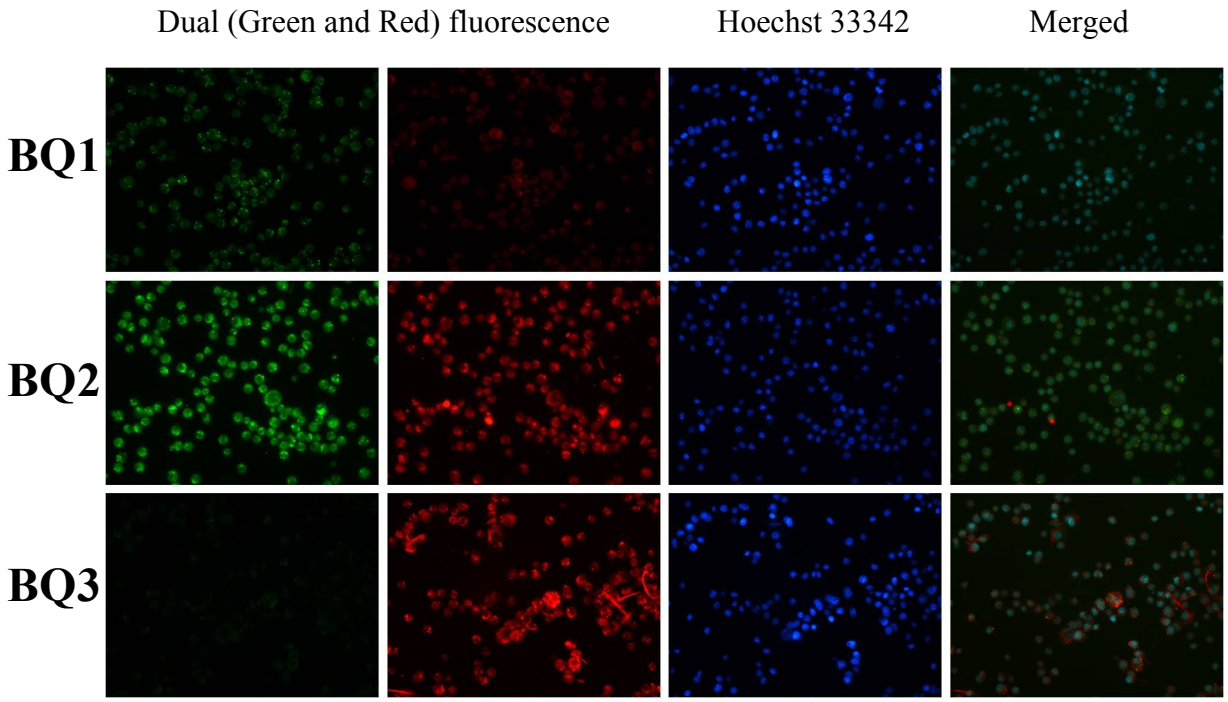

Figure S35: Fluorescence images of live DL cells with **BQ1**–**BQ3** and co-stained with Hoechst 33342. The images from left to right show staining with the **BQ1**–**BQ3** followed by nucleus staining with Hoechst 33342 and merged.

Table S1. Selected crystallographic parameters for **BQ1**–**BQ4**.

Crystal data	**BQ1**	**BQ2**	**BQ3**	**BQ4**
Empirical formula	$C_{19}H_{14}BF_2N_3S$	$C_{23}H_{23}BF_2N_3S$	$C_{20}H_{16}B\ F_2N_3OS$	$C_{18}H_{11}BClF_2N_3$
Crystal system	Monoclinic	Monoclinic	Monoclinic	Monoclinic
Space group	$P2_1/c$	$P2_1/n$	$P2_1/c$	$P2_1/c$
a (Å)	13.4997(9)	16.3271(1)	10.5497(2)	9.7361(2)
b (Å)	13.9995(7)	8.3270(4)	19.995(3)	14.5464(2)
c (Å)	10.1052(6)	16.9926(8)	9.2865(2)	12.2140(2)
α (°)	90.00	90.00	90.00	90.00
β (°)	111.458(8)	109.759(3)	104.898(15)	111.146(2)
γ (°)	90.00	90.00	90.00	90.00
V (Å^3)	1777.39(2)	2174.2(2)	1893.0(5)	1613.33(5)
Z	4	4	4	4
F(000)	752.0	884.0	816	720
ρ_{calc} (Mg m^{-3})	1.365	1.290	1.387	1.456
T (K)	293 (2)	296(2)	293(2)	150(2)
μ (mm^{-1})	1.855	0.180	0.206	2.336
refln collected	3125	4629	4147	3131

GOF on F^2	1.056	1.116	1.035	1.043
final R1 on observed data	0.0520	0.0450	0.0688	0.0461
final wR2 on observed data	0.1455	0.1410	0.1799	0.1259

Table S2. Selected bond distances (a) and angles (b) in **BQ1**–**BQ3**.

(a)

Bond Length (Å)	**BQ1**	**Bond Length (Å)**	**BQ2**	**Bond Length (Å)**	**BQ3**
S1-C11	1.762(2)	S1-C11	1.7662(2)	S1-C11	1.776(3)
S1-C19	1.784(3)	S1-C19	1.772(2)	S1-C19	1.796(4)
N1-B1	1.545(3)	N1-B1	1.541(2)	N1-B1	1.541(6)
N2-B1	1.539(3)	N2-B1	1.547(2)	N2-B1	1.552(5)
N3-C11	1.307(3)	N3-C11	1.308(2)	N3-C11	1.311(4)
N3-C12	1.372(3)	N3-C12	1.373(2)	N3-C12	1.378(4)
C10-C5	1.491(3)	C10-C5	1.491(2)	C10-C5	1.482(4)

(b)

Bond Angle (°)	**BQ1**	**Bond Angle (°)**	**BQ2**	**Bond Angle (°)**	**BQ3**
F1-B1-F2	109.3(2)	F1-B1-F2	109.09(14)	F1-B1-F2	108.9(3)
N2 B1 N1	106.22(2)	N2 B1 N1	105.61(1)	N2 B1 N1	106.3(3)
C4-C5-C6	120.33(2)	C4-C5-C6	120.64(2)	C4-C5-C6	119.9(3)
C6-C5-C10	119.71(2)	C6-C5-C10	119.60(2)	C6-C5-C10	119.0(3)
C4-C5-C10	119.97(2)	C4-C5-C10	119.75(2)	C4-C5-C10	121.2(3)
C11-C10-C5	121.26(2)	C11-C10-C5	120.33(1)	C11-C10-C5	122.6(3)
C18-C10-C5	120.64(2)	C18-C10-C5	122.01(2)	C18-C10-C5	119.9(3)

C11-S1-C19	101.83(1)	C11-S1-C19	101.46(9)	C11-S1-C19	102.12(2)

References:

1. R. S. Singh, M.Yadav, R. K. Gupta, R. Pandey and D. S. Pandey, *Dalton Trans.*, 2013, **42**, 1696–1707.
2. G. M. Sheldrick, *SHELXL-97, Program for X-ray Crystal Structure Refinement*; Gottingen University: Gottingen, Germany, 1997. (b) G. M. Sheldrick, *SHELXS-97, Program for X-ray Crystal Structure Solution*; Gottingen University: Gottingen, Germany, 1997.
3. (a) A. L. Spek, *PLATON, A Multipurpose Crystallographic Tools* Utrecht University, Utrecht, The Netherlands, 2000. (b) A. L. Spek, *Acta Crystallogr. A*, 1990, **46***,* C31.
4. (a) Y. Zhou, Y. Xiao, D. Li, M. Fu and X. Qian, *J. Org. Chem.*, 2008, **73**, 1571–1574. (b) P. E. Burrows, Z. Shen, V. Bulovic, D. M. McCarty, S. R. Forrest, J. A. Cronin and M. E. Thompson, *J. Appl. Phys.*, 1996, **79**, 7991–8006.
5. M. J. Frisch, G. W. Trucks, H. B. Schlegel, G. E. Scuseria, M. A. Robb, J. R. Cheeseman, G. Scalmani, V. Barone, B. Mennucci, G. A. Petersson, H. Nakatsuji, M. Caricato, X. Li, H. P. Hratchian, A. F. Izmaylov, J. Bloino, G. Zheng, J. L. Sonnenberg, M. Hada, M. Ehara, K. Toyota, R. Fukuda, J. Hasegawa, M. Ishida, T. Nakajima, Y. Honda, O. Kitao, H. Nakai, T. Vreven, J. A. Montgomery, Jr., J. E. Peralta, F. Ogliaro, M. Bearpark, J. J. Heyd, E. Brothers, K. N. Kudin, V. N. Staroverov, R. Kobayashi, J. Normand, K. Raghavachari, A. Rendell, J. C. Burant, S. S. Iyengar, J. Tomasi, M. Cossi, N. Rega, J. M. Millam, M. Klene, J. E. Knox, J. B. Cross, V. Bakken, C. Adamo, J. Jaramillo, R. Gomperts, R. E. Stratmann, O. Yazyev, A. J. Austin, R. Cammi, C. Pomelli, J. W. Ochterski, R. L. Martin, K. Morokuma, V. G. Zakrzewski, G. A. Voth, P. Salvador, J. J. Dannenberg, S. Dapprich, A. D. Daniels, Ö. Farkas, J. B. Foresman, J. V. Ortiz, J. Cioslowski and D. J. Fox, *Gaussian 09, revision A.1, Gaussian, Inc., Wallingford, CT,* 2009.

6. D. D. Perrin, W. L. F. Armango and D. R. Perrin, *Purification of laboratory Chemicals,* Pergamon: Oxford, U.K. 1986.